Title

Systematic Genetic Screen for Transcriptional Regulators of the Candida albicans White-Opaque Switch.

Journal

Genetics, 203(4)

ISSN

0016-6731

Authors

Lohse, Matthew B
Ene, Iuliana V
Craik, Veronica B
et al.

Publication Date

2016-08-01

DOI

10.1534/genetics.116.190645

Peer reviewed

Systematic Genetic Screen for Transcriptional Regulators of the *Candida albicans* White-Opaque Switch

Matthew B. Lohse,*,[1] Iuliana V. Ene,[†] Veronica B. Craik,* Aaron D. Hernday,[‡] Eugenio Mancera,* Joachim Morschhäuser,[§] Richard J. Bennett,[†] and Alexander D. Johnson*,,[2]**

*Department of Microbiology and Immunology and **Department of Biochemistry and Biophysics, University of California, San Francisco, California 94158, [†]Department of Molecular Microbiology and Immunology, Brown University, Providence, Rhode Island 02912, [‡]Department of Molecular and Cell Biology, University of California, Merced, California 95343, and [§]Institut für Molekulare Infektionsbiologie, Universität Würzburg, D-97080, Würzburg, Germany

ABSTRACT The human fungal pathogen *Candida albicans* can reversibly switch between two cell types named "white" and "opaque," each of which is stable through many cell divisions. These two cell types differ in their ability to mate, their metabolic preferences and their interactions with the mammalian innate immune system. A highly interconnected network of eight transcriptional regulators has been shown to control switching between these two cell types. To identify additional regulators of the switch, we systematically and quantitatively measured white–opaque switching rates of 196 strains, each deleted for a specific transcriptional regulator. We identified 19 new regulators with at least a 10-fold effect on switching rates and an additional 14 new regulators with more subtle effects. To investigate how these regulators affect switching rates, we examined several criteria, including the binding of the eight known regulators of switching to the control region of each new regulatory gene, differential expression of the newly found genes between cell types, and the growth rate of each mutant strain. This study highlights the complexity of the transcriptional network that regulates the white–opaque switch and the extent to which switching is linked to a variety of metabolic processes, including respiration and carbon utilization. In addition to revealing specific insights, the information reported here provides a foundation to understand the highly complex coupling of white–opaque switching to cellular physiology.

KEYWORDS white-opaque switching; transcriptional regulation; transcription networks; transcriptional circuits; *Candida albicans*

THE fungal species *Candida albicans* is normally a harmless component of the human microbiome, but it can also cause life threatening bloodstream infections, particularly in immunocompromised patients. *C. albicans* has the unusual ability to switch between two cell types, named "white" and "opaque," each with distinct cellular and colony morphologies (Figure 1, A and B) (Slutsky *et al.* 1987; Soll *et al.* 1993; Johnson 2003; Lohse and Johnson 2009; Soll 2009; Morschhäuser 2010). Each cell type is heritable for many cell divisions, and switching from one form to the other occurs without any change in the primary DNA sequence of the genome. Under standard laboratory conditions, switching between the two cell types occurs stochastically with approximately one switching event every 10^4 cell divisions, although certain environmental cues, such as elevated temperatures, can cause mass switching from one cell type to the other (Rikkerink *et al.* 1988; Huang *et al.* 2009, 2010; Lohse *et al.* 2013). Expression of ~20% of the genes in *C. albicans* is differentially regulated between the two cell types (Lan *et al.* 2002; Tuch *et al.* 2010) and, as a result, the white and opaque forms differ in their ability to mate (Miller and Johnson 2002), their metabolic preferences (Lan *et al.* 2002), and their interactions with the innate immune system (Kvaal *et al.* 1997, 1999; Geiger *et al.* 2004; Lohse and Johnson 2008; Sasse *et al.* 2013). Furthermore, the two cell types differ in their ability to respond to other environmental signals such as those that induce filamentous growth (Si *et al.* 2013).

doi: 10.1534/genetics.116.190645
Manuscript received April 19, 2016; accepted for publication May 23, 2016; published Early Online June 6, 2016.
Supplemental material is available online at www.genetics.org/lookup/suppl/doi:10.1534/genetics.116.190645/-/DC1.
[1]Present address: Department of Biology, BioSynesis, San Francisco, CA 94114.
[2]Corresponding author: Department of Microbiology and Immunology, University of California, San Francisco, Box 2200, 600 16th St., San Francisco, CA 94143. E-mail: ajohnson@cgl.ucsf.edu

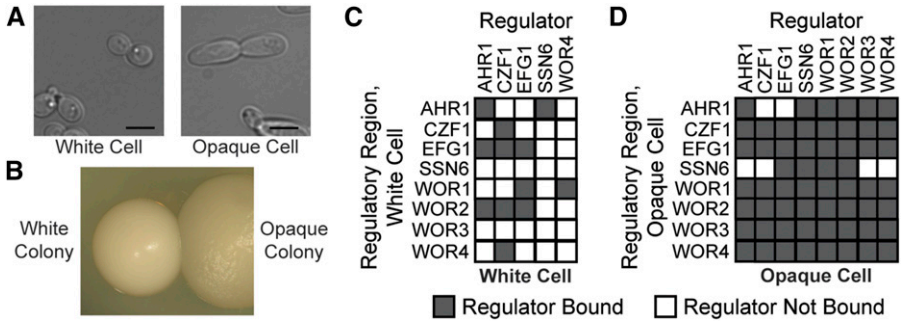

Figure 1 Known white–opaque regulatory circuitry. (A) Typical white and opaque cells grown in liquid culture. Bar, 5 μm. (B) Typical white (left) and opaque (right) colonies. (C and D) Regulatory circuit in (C) white and (D) opaque cells based on binding events identified in previously published ChIP studies of key regulators of switching (Zordan *et al.* 2007; Hernday *et al.* 2013, 2016; Lohse *et al.* 2013; Lohse and Johnson 2016). The charts indicate which regulators were enriched at the control region of each regulator. Dark boxes indicate binding of the regulator at a given regulatory region, while empty boxes indicate a lack of significant binding.

White–opaque switching has previously been shown to be regulated by eight different transcriptional regulators (Figure 1, C and D). Five of these (Wor1, Wor2, Wor3, Wor4, and Czf1) are important for the establishment and/or maintenance of the opaque cell type, whereas the other three (Efg1, Ahr1, and Ssn6) contribute to the stability of the white cell type (Sonneborn *et al.* 1999; Srikantha *et al.* 2000, 2006; Huang *et al.* 2006; Zordan *et al.* 2006, 2007; Vinces and Kumamoto 2007; Wang *et al.* 2011; Hernday *et al.* 2013, 2016; Lohse *et al.* 2013; Lohse and Johnson 2016). Wor1, which is highly upregulated in the opaque cell type, is often considered the "master regulator" of the switch; its expression is necessary for both the establishment and the maintenance of the opaque cell type (Huang *et al.* 2006; Srikantha *et al.* 2006; Zordan *et al.* 2006, 2007). Wor2, Wor3, Wor4, and Czf1 contribute either to the establishment (Czf1, Wor3, and Wor4) or the maintenance (Wor2 and Wor4) of the opaque cell type in a Wor1-dependent manner (Vinces and Kumamoto 2007; Zordan *et al.* 2007; Hernday *et al.* 2013; Lohse *et al.* 2013; Lohse and Johnson 2016). All of the aforementioned genes, except *WOR4*, are transcriptionally upregulated in the opaque cell type (Lan *et al.* 2002; Tuch *et al.* 2010; Hernday *et al.* 2013). *EFG1*, which is upregulated in the white cell type, stabilizes the white cell type, largely through the repression of *WOR1* expression (Stoldt *et al.* 1997; Sonneborn *et al.* 1999; Zordan *et al.* 2007; Hernday *et al.* 2013). Ahr1, which is not differentially regulated between the two cell types, helps repress the white-to-opaque switch in an Efg1-dependent manner (Wang *et al.* 2011; Hernday *et al.* 2013). Ssn6, which is also not differentially regulated between the two cell types, represses white-to-opaque switching as well as a portion of the opaque cell transcriptional program in white cells (Hernday *et al.* 2016). Together, these transcriptional regulators act as part of two mutually exclusive, self-perpetuating positive transcriptional feedback loops. It has been proposed that these feedback loops form the basis for the two cell types and the stability of each cell type through many cell divisions (Zordan *et al.* 2007; Sriram *et al.* 2009). In addition to these eight regulators, recent studies have identified several additional regulators with more subtle effects on switching (*i.e.*, Flo8, Lys143, and Ofi1); however, their relationship to the core regulatory circuits is not fully understood (Du *et al.* 2012, 2015; Pérez *et al.* 2014).

Although a considerable amount is known about the regulation of white–opaque switching, the identification of the key transcriptional regulators described above was largely the result of informed guesses (based on genome-wide expression data) or fortuitous observations of gene deletions being studied for different reasons. Thus far, there has been no systematic attempt to identify transcriptional regulators that affect switching between the white and opaque cell types. Likewise, there has been no unbiased screen for transcriptional regulators that are required for the full establishment of the opaque phenotype, regardless of whether or not they affect switching rates. One reason for this lack of information is that the standard laboratory strain of *C. albicans* (SC5314) is a *MTL***a**/α strain, where white-to-opaque switching is blocked by the action of the **a**1–α2 heterodimer (Miller and Johnson 2002); the large-scale gene deletion libraries constructed for *C. albicans* utilized this strain, so it was not possible to directly screen for mutations that affect switching rates (Homann *et al.* 2009; Noble *et al.* 2010).

To systematically identify transcriptional regulators involved in white–opaque switching, we constructed a comprehensive *C. albicans* transcriptional regulator deletion library in a strain background that readily undergoes white–opaque switching (*MTL***a**/Δ). By screening each member of the library in a quantitative manner, we identified many regulators (most of which were previously unreported) whose deletion affects white–opaque switching frequencies in one or both directions. Further examination of the effects of these deletions on growth rate and cellular morphology allowed the identification of mutants with effects specific to the white cell type or the opaque cell type. The results show that the white–opaque switch is highly integrated into the global *C. albicans* transcriptional network, indicating that switching is physiologically linked with many other aspects of *C. albicans* biology, including carbon utilization, nitrogen utilization, pH response, and filamentation.

Materials and Methods

Media

All strains were grown on synthetic complete media supplemented with 2% glucose, amino acids, and 100 μg/ml uridine (SD+aa+Uri) at room temperature (~22°) unless otherwise noted.

Strain construction

A list of oligonucleotides used in this study can be found in Supplemental Material, Table S1. A list of plasmids used in this study can be found in Table S2. A list of strains used in this study can be found in Table S3.

Deletion mutants in the **a**/α cell type have been previously reported for 192 of the transcriptional regulators. In brief, **a**/α mutants TF1–TF165 were reported in Homann *et al.* (2009), TF166–TF178 and TF180–TF183 in Fox *et al.* (2014), TF185 in Fox *et al.* (2015), and TF186–TF192 in Noble *et al.* (2010). These mutants were constructed in the SN152 (**a**/α *his1 leu2 arg4*) background (Noble and Johnson 2005). Mutants TF1–TF165, TF178, TF180, TF183, and TF186–TF192 were converted to the switching capable **a**/Δ background using pJD1 (Lin *et al.* 2013) to delete the α-copy of the mating-type-like (*MTL*) locus. Mating types of the resulting strains were verified by colony PCR against both the **a** and α *MTL* loci. A small number of mutants (TF166–TF169, TF171–TF173, TF175, TF177, TF182, and TF185) were made independently in the RZY47 (**a**/**a** *his1 leu2*) strain background (Zordan *et al.* 2006) using the *HIS1* and *LEU2* cassettes (Noble and Johnson 2005) in parallel with the construction of the previously reported **a**/α mutants. The **a**/**a** mutants for TF174 and TF179 were also constructed in the RZY47 background. The previously reported **a**/**a** or **a**/Δ mutants of TF176 (*wor1*) (Zordan *et al.* 2006), TF170 (*wor3*) (Lohse *et al.* 2013), and TF181 (*wor4*) (Lohse and Johnson 2016) were also incorporated into the library.

The TF193 (*std1*) mutant was constructed in the RZY47 background using the *HIS1* and *LEU2* cassettes (Noble and Johnson 2005). The TF194–TF197 mutants (*hap42*, *iro1*, *hap41*, and *hac1*) were initially constructed in the SN152 (**a**/α *his1 leu2 arg4*) background using the *HIS1* and *LEU2* cassettes and then converted to the **a**/Δ background using pJD1. Correct chromosomal integration and orientation of each marker and loss of the ORF were verified by colony PCR. It was not possible to verify the 5′ *LEU2* cassette flank of the *hap41* mutant, but we verified the absence of the *HAP41* ORF by colony PCR with three independent sets of PCR primers.

Ectopic expression of a subset of regulators was achieved using a previously described system that allows induction of gene expression in *C. albicans* by the addition of tetracycline (Park and Morschhäuser 2005; Ramírez-Zavala *et al.* 2008). The tetracycline-inducible gene cassette pNIM1 or pNIM6 is flanked by *Sal*I and *Bgl*II restriction sites (also compatible with *Xho*I and *Bam*HI, respectively) allowing the ORFs of interest to be substituted for the *Ca*GFP reporter gene in a single cloning step (Park and Morschhäuser 2005; Ramírez-Zavala *et al.* 2008). pNIM1 and pNIM6 differ only in the presence of the *TEF3* (pNIM6) or *ACT1* (pNIM1) terminators downstream of the *Ca*GFP reporter gene. The amplified ORFs of interest were cloned into either the pNIM1 or the pNIM6 vector, which was then digested with *Apa*I and *Sac*II and transformed into the CAY616 strain (see Table S2 for a list of which plasmid was used for each gene). Transformants were positively selected on nourseothricin (*SAT1*$^+$) and correct integration was verified by colony PCR against the 5′ and 3′ flanks. The pNIM1 vector containing *Ca*GFP was also transformed into the CAY616 strain and efficient tetracycline-inducible expression was verified in this strain by monitoring GFP expression. Two independently transformed strains showed efficient GFP expression upon addition of 50 μg/ml doxycycline to the growing medium as confirmed by fluorescent microscopy. The sequence of the cassette contained in pNIM1 can be found in GenBank under accession no. DQ090840.

Strains excluded from switching assays

It was not possible to convert mutant TF184 (*gcn4*) to the **a**/Δ background due to a lack of suitable markers; therefore, it was not tested in the various screens reported here and is not counted toward the 196 mutants tested. Hyperfilamentation of TF117 (*tup1*) and TF125 (*nrg1*) as well as septation defects of TF59 (*ace2*) prevented determination of either white-to-opaque or opaque-to-white switching rates. Both the TF113 (*rbf1*) and TF121 (*ssn6*) mutants appear heavily biased to, or even locked in, the opaque cell type, and as such it was not possible to determine white-to-opaque switching rates. We were unable to isolate opaque cells for TF56 (*wor2*), TF175 (*flo8*), TF176 (*wor1*), and TF181 (*wor4*), and as such could not determine opaque-to-white switching rates for these strains. The TF137 (*bcr1*) mutant is hyperfilamentous in the opaque cell type, preventing us from determining its opaque-to-white switching rate. We note that it was not possible to obtain a complete deletion of TF182 (*CBF1*), so in this case, the heterozygous deletion (*CBF1*/*cbf1*) was tested. Further details of strains that could not be tested in specific assays or that are excluded from specific analyses are included in File S1, Supplemental Materials and Methods.

White-to-opaque and opaque-to-white switching assays

The white-to-opaque and opaque-to-white switching screens used a variation of the previously reported switching assay (Miller and Johnson 2002; Zordan *et al.* 2007). Blind identifications were assigned to strains during the recovery from frozen glycerol stocks on SD+aa+Uri plates. These blind identifications were maintained during the plating and scoring process. Following recovery from glycerol stocks, plates were grown for 7 days at room temperature (~22°). Three to five colonies of the appropriate cell type, without visible sectors, were resuspended in water, diluted, plated on SD+aa+Uri (six plates per strain), and allowed to grow for 7 days at room temperature. Five replicates of wild type and ~20–25 deletion strains were screened on a given day. Plates were scored, keeping track of (A) colonies of the starting cell type, (B) colonies of the starting cell type with one or more sectors, and (C) colonies of the other cell type. We have calculated the switching frequency as (B + C)/(A + B + C). When no

switching events were detected for a strain, we have set the switching frequency to 1/(total number of colonies counted on all of the plates for that strain) to aid in visualization. The switching frequency for a given strain was then normalized to the average switching frequency of the five wild-type replicates from the same day. We note that we were able to obtain opaque cell isolates for several strains that did not switch in this assay by examining a larger number of colonies outside the context of the screen. Due to issues described above, we could not obtain white-to-opaque switching rates for TF59 (*ace2*), TF113 (*rbf1*), TF117 (*tup1*), TF121 (*ssn6*), and TF125 (*nrg1*). We could not obtain opaque-to-white switching rates for TF56 (*wor2*), TF59 (*ace2*), TF117 (*tup1*), TF125 (*nrg1*), TF137 (*bcr1*), TF175 (*flo8*), TF176 (*wor1*), and TF181 (*wor4*). Switching rates for all strains tested are included in File S2. The switching assays for Figure 6 are described in File S1, Supplemental Materials and Methods.

A full description of the statistical analyses performed for the switching assays is provided in File S1, Supplemental Materials and Methods. We used Welch's *t*-test (two tailed) to compare the switching rates for the individual mutant plates (usually six plates) to the switching rates for the individual plates from the five wild-type controls (usually 30 plates) from the same day. We evaluated each mutant separately for the white-to-opaque and opaque-to-white assays. When no switching events were detected on a given plate, we set the switching frequency of that plate to 1/(number of colonies counted on that plate) for the purposes of this analysis. The raw *P*-values for each mutant are included in File S2. We used the Benjamini–Hochberg procedure (BH step-up procedure) with $\alpha = 0.05$ to correct for multiple comparisons; at this threshold all mutants with greater than threefold effects on white-to-opaque or opaque-to-white switching were significant.

Ectopic expression assays

Ectopic expression switching assays were performed similarly to the protocol described above with the following modifications. *C. albicans* cells were grown as described above, cultured overnight, and the following day, cells were diluted to a density of $OD_{600} = 0.1$ in 4 ml of SD+aa+Uri and supplemented with 50 μg/ml doxycycline (+dox). After 4 hr of growth, ~100–300 cells were plated on SD+aa+Uri plates top spread with 50 μg/ml doxycycline (assuming a ~20-ml agar volume). Quantification of switching events was carried out as above following 7–8 days of growth at room temperature. To determine the effects of ectopic expression of target genes on white–opaque switching, rates were compared to untreated controls (−dox). Between three and six independent experiments were performed for each strain in both the white-to-opaque and opaque-to-white directions.

Statistical analysis of ectopic switching assays was performed as follows. For any assay where no switching events were detected, the switching rate was set to 1/(number of colonies scored) in order to allow for a comparison of the +dox and −dox rates. For each replicate, we then determined the +dox and −dox switching rates and then calculated the ratio of the +dox assay rate to the −dox assay rate. In Table S4, we report the median of the ratios for the three to six independent experiments for each strain. We also performed a paired *t*-test (two tailed) comparing the switching rates of the +dox repeats to the −dox repeats. We have defined regulators affecting switching in this assay as those with at least a twofold change in switching rates and $P < 0.1$ (paired *t*-test, two tailed).

Comparisons between data sets

Unless otherwise noted, comparisons in the text use the following sets of regulators. Comparisons between white-to-opaque and opaque-to-white switching rates used the set of regulators with at least threefold effects in either cell type. Switching comparisons with nonswitching data sets use the set of regulators whose deletion had at least 10-fold effects on switching (either in one direction or both directions). Comparisons between switching rates and growth rate comparisons use mutants with at least a 20% growth rate decrease relative to wild type and at least fivefold effects on switching. Growth rate comparisons between cell types use mutants that have growth rates for both cell types and with at least a 20% growth rate decrease relative to wild type. When comparing a given metric in two directions (*e.g.*, growth rates in white cells and opaque cells) or when comparing two metrics (*e.g.*, growth rates in white cells and white-to-opaque switching rates), we limited comparisons to those regulators that had values for both conditions unless otherwise noted. Specific details of the various data set comparisons are provided in File S1, Supplemental Materials and Methods and Supplemental Results. A summary of all of these comparisons is included in Table S5.

Transcriptional profiling data are taken from previously reported RNA-sequencing (RNAseq) experiments (Tuch *et al.* 2010) and known regulator binding (Ahr1, Czf1, Efg1, Ssn6, Wor1, Wor2, Wor3, and Wor4) combines data from a number of studies (Zordan *et al.* 2007; Hernday *et al.* 2013, 2016; Lohse *et al.* 2013; Lohse and Johnson 2016). We used a twofold differential expression threshold for comparisons to the transcriptional data set and binding by at least one regulator for comparisons to the ChIP binding data sets. Binding of regulators in white and opaque cells were considered separately. Correlation coefficients (both Pearson's *r* and Spearman's rho) were calculated using GraphPad Prism 6. The calculations for determining the enrichment of a given data set predicting a second data set, relative to that expected by chance, are discussed in File S1, Supplemental Materials and Methods.

Growth rate assays

Room temperature SD+aa+Uri overnight cultures were started from white or opaque colonies of each strain. The following morning, we diluted overnight cultures to a density of $OD_{600} = 0.01$ in 100 μl of SD+aa+Uri. Growth curve assays were performed on a Tecan Infinite M1000 Pro at a temperature of 25°. Absorbance was measured for five locations in each well every 15 min for 45 hr (180 cycles); the plate was shaken continuously between reads. This setup

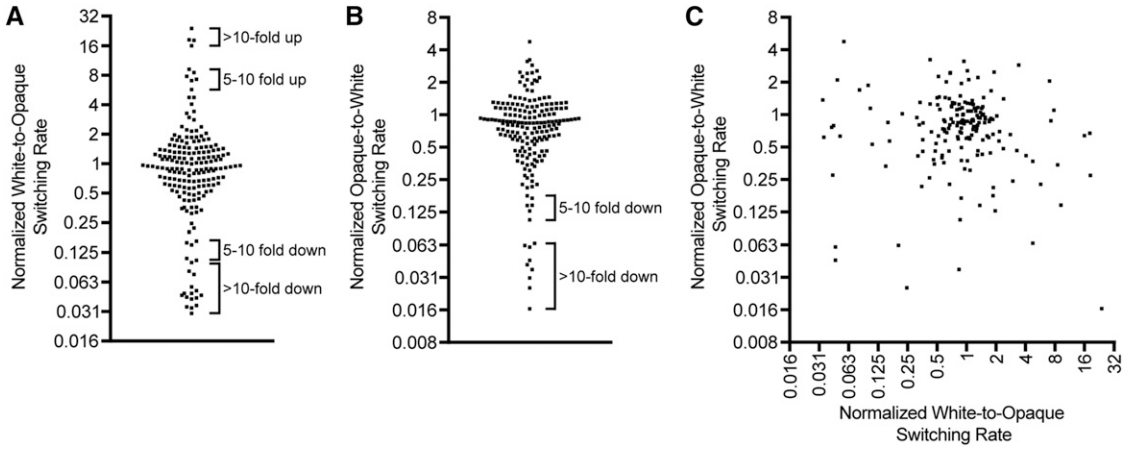

Figure 2 Identification of new regulators that affect white-to-opaque or opaque-to-white switching. (A) White-to-opaque switching frequencies for 191 regulators, normalized to the average of five wild-type switching assays performed the same day. (B) Opaque-to-white switching frequencies for 188 regulators, normalized to the average of five wild-type switching assays from the same day. (C) Comparison of normalized white-to-opaque and opaque-to-white switching rates for 186 regulators (Pearson's *r*, −0.15; Spearman's rho, −0.04). A value of 1 represents switching at the wild-type rate, values <1 reflect reduced switching, and values >1 reflect increased switching. Axes are plotted on a $\log_2$ scale.

allowed cells to recover from the dilution, enter log phase growth, and to eventually reach saturation. Three replicates on the same day were performed for each sample and wild-type samples were included on each plate to allow for comparisons between experiments.

Maximum growth rates (1/hr) were estimated as the maximum slope of a smooth fit to the raw data using the R/Bioconductor cellGrowth package as described by Gagneur *et al.* (2013). For each strain, three growth curves (corresponding to the three wells) were independently generated and analyzed, and the average of these replicates was used to determine the corresponding maximum growth rate of the strain. The maximum growth rates for each deletion mutant were then normalized to the maximum growth for the wild-type sample from the same day to allow for easier comparisons between days.

A full description of the statistical analyses performed for the growth rate assays is provided in File S1, Supplemental Materials and Methods. We used Welch's *t*-test (two tailed) to compare the growth rates of the individual mutant wells (usually three wells) to the growth rates of the individual wild-type wells (usually three wells) from the same day. We evaluated each mutant separately for the white and opaque cell growth rate assays. The raw *P*-values for each mutant are included in File S2. We used the BH step-up procedure with $\alpha = 0.05$ to correct for multiple comparisons; at this threshold all but one of the mutants with 20% effects on white cell growth rates and all of the mutants with 20% effects on opaque cell growth rates were significant.

Microscopy

Cells used for microscopy were taken from overnight cultures (SD+aa+Uri at room temperature, ~22°) that were started from representative colonies. Multiple images of each opaque strain were taken on 2 days (between three and five images per day). Between 15 and 30 strains were imaged on a typical day using a Zeiss Axiovert 200M microscope. Two individuals independently scored each repeat of the opaque cell library for abnormalities. We then focused on strains identified by both individuals in both repeats and repeated the assay for the white cell versions of each strain that displayed an abnormal opaque cell phenotype.

Quantitative PCR

Samples for quantitative PCR (qPCR) were prepared as follows. Room temperature SD+aa+Uri overnights were started from 5- to 7-day-old colonies. Cultures were diluted to $OD_{600} = 0.2$ in the morning and allowed to grow to an OD_{600} of ~0.8 at 25°. The equivalent of 10 ml at $OD_{600} = 1$ (1 ml at $OD_{600} = 1$ contains $\sim 2 \times 10^7$ cells) was harvested for each culture. Cells were pelleted, the supernatant discarded, and the pellet flash frozen in liquid nitrogen prior to storage at −80°. Cells from each culture were also plated on SD+aa+Uri plates and grown for 7 days at room temperature to verify the cell type composition and to ensure that results were not biased by larger than expected numbers of opaque cells. RNA was extracted from cell pellets using the Ambion RiboPure Yeast Kit with the DNase I treatment step. Superscript II RT was used for complementary DNA (cDNA) synthesis following the manufacturer's recommendations for oligo dT. We used Power SYBR Green Mix (Life Tchnologies) for all qPCR reactions. Three +reverse transcriptase (RT) and one −RT reaction were run for each strain; 5 μl of a 1:100 dilution was used in each well. A 1:10 dilution of an equal volume mixture of all +RT reactions was used as the starting point for the standard curve, which consisted of six 1:4 dilutions from the starting sample. The *DYN1* gene was used as a control.

Data availability

Strains and plasmids are available on request. File S2 contains the normalized switching and growth rates for all mutant

strains tested in this study, as well as the statistical analyses of the switching rate and growth rate screens.

Results

Construction of a transcriptional regulator deletion library in a C. albicans strain competent for white-opaque switching

We previously reported a comprehensively vetted *C. albicans* transcription factor deletion mutant library that was constructed in the **a**/α mating type background of strain SC5314 (Homann *et al.* 2009); in this background *WOR1* is repressed by the a1–α2 heterodimer and the strain is therefore locked in the white cell type. We utilized an *MTL* locus deletion cassette to convert—one mutant at a time—the **a**/α strain library to the **a**/Δ mating type, which is capable of white-to-opaque switching because the α2 gene is absent (Miller and Johnson 2002). To the 165 strains from the original **a**/α library, we added 26 transcription regulator mutants whose construction in the **a**/α background has been previously reported (Homann *et al.* 2009; Noble *et al.* 2010; Fox *et al.* 2014, 2015) as well as an additional five new transcription regulator deletion mutants. The expanded library (detailed in *Materials and Methods* and File S1) thus consists of 196 deletion mutants, a list of which is given in Table S3. We arbitrarily chose 10 genes and constructed independent homozygous deletion mutants and observed that 9 of the 10 mutants showed a range of phenotypes identical to the original isolate. This frequency of reproducibility is similar to that observed for other phenotypes during the vetting of the initial **a**/α library (143 of 155 mutants with two independent isolates have similar phenotypes) (Homann *et al.* 2009).

Identification of new regulators of white-opaque switching

An initial screen of the 196 transcriptional regulator mutant strains was carried out to identify regulators with effects on white-to-opaque switching. The white-to-opaque switching rate was calculated by determining the fraction of colonies with one or more opaque sectors for each mutant and normalizing it to that observed in wild type colonies grown on the same day (see *Materials and Methods* for a more detailed description). We could determine white-to-opaque switching rates for 191 of the 196 mutants (see *Materials and Methods* and File S1 for full explanations of strains examined). Four of these strains exhibited >10-fold increase in white-to-opaque switching (relative to wild type) and 16 strains exhibited a >10-fold reduction in white-to-opaque switching (Figure 2A and Table 1). This list included six of the previously identified regulators of white–opaque switching (Czf1, Efg1, Flo8, Wor1, Wor2, and Wor4) along with 14 previously unreported regulators, including Gal4, Hap2, Hap31, Hcm1, Mig1, Ndt80, Rap1, and Rpn4. We also identified an additional 11 deletion mutants with less severe effects (five- to 10-fold) on white-to-opaque switching, 10 of which had not previously been linked to switching. Two additional strains (*rbf1* and *ssn6*) were unable to form white colonies and, in a sense, could be considered to have a greatly increased white-to-opaque switching rate.

We were able to isolate opaque cells for 188 of the 196 deletion mutants in this library (see *Materials and Methods* and

Table 1 List of mutants with fivefold or greater effects on white-to-opaque or opaque-to-white switching frequencies

TFKO number	Name	Normalized white-to-opaque switching frequency	Normalized opaque-to-white switching frequency
TF132	AHR1	1.956	0.128
TF074	ASG1	0.046	0.045
TF112	ASH1	0.835	0.037
TF068	CRZ1	1.861	0.177
TF070	CTA4	0.883	0.168
TF061	CUP9	4.743	0.065
TF104	CZF1	0.046	0.060
TF155	DAL81	0.163	0.571
TF156	EFG1	23.994	<0.016
TF152	FGR15	0.056	4.777
TF175	FLO8	<0.036	N/A[a]
TF045	GAL4	<0.042	0.765
TF144	GIS2	0.861	0.106
TF021	GRF10	1.368	0.144
TF101	GZF3	0.081	1.697
TF087	HAP2	<0.035	0.618
TF079	HAP31	0.044	0.791
TF196	HAP41	0.104	1.143
TF093	HAP5	0.150	0.332
TF036	HCM1	18.345	0.273
TF103	HFL1	<0.048	2.106
TF185	INO2	<0.043	0.275
TF161	LYS143	7.253	0.878
TF065	MAC1	0.051	0.633
TF107	MIG1	<0.034	1.370
TF095	NDT80	0.099	1.868
TF102	orf19.2961	7.024	2.050
TF019	orf19.3928	5.711	0.226
TF168	orf19.5210	0.157	0.847
TF123	orf19.6888	0.201	0.062
TF190	orf19.7098	7.769	1.099
TF158	RAP1	15.959	0.639
TF113	RBF1	N/A[b]	<0.031
TF058	RCA1	0.109	0.531
TF003	RPN4	18.178	0.672
TF121	SSN6	N/A[b]	<0.041
TF162	STP2	9.184	0.145
TF176	WOR1	<0.048	N/A[a]
TF056	WOR2	<0.030	N/A[a]
TF181	WOR4	<0.075	N/A[a]
TF024	ZCF21	0.246	0.025
TF031	ZCF25	8.485	0.342

White-to-opaque and opaque-to-white switching frequencies, normalized to the average of five wild-type switching assays performed on the same day, are presented for each mutant. When no switching events were detected for a strain in the screen, the switching frequency is indicated as <1 divided by the number of colonies counted. Strains for which we could not determine a switching frequency are indicated. The switching rates of all strains with greater than a fivefold effect on white-to-opaque or opaque-to-white switching were significantly different from wild type (Welch's *t*-test (two tailed) with BH step-up procedure, α = 0.05, see File S1 for details).

[a] No opaque isolate.

[b] No white isolate.

Table 2 Processes with regulators whose deletion affects white-opaque switching

Process	White-to-opaque switching	Both directions	Opaque-to-white switching
Filamentation	FLO8[a] RAP1	CZF1, EFG1, FGR15, HAP5	ASH1, GRF10, RBF1[a]
Carbon utilization	GAL4, HAP2, HAP31, MIG1, ZCF7	HAP5	
Nitrogen utilization	DAL81, GZF3	STP2	
pH response	HAP2, WAR1	HAP5, STP2	CRZ1, CTA4
Response to metal/copper	GZF3, HAP2, HAP31, MAC1, NDT80, orf19.2961	HAP5	CAP1, SEF2, ZCF31

Selected processes with multiple regulators whose deletion affects either white-to-opaque or opaque-to-white switching at least threefold when deleted. The direction(s) of each regulator's effect is indicated.
[a] It was only possible to screen switching in one direction for this regulator.

File S1 for details of the eight strains that did not switch to opaque), allowing us to screen for effects of the deletions on switching in the reverse direction, that is, from opaque to white. Of these 188 mutants, 9 had a 10-fold or greater reduction in opaque-to-white switching, of which six regulators (Asg1, Ash1, Cup9, orf19.6888, Rbf1, and Zcf21) had not previously been linked to switching (Figure 2B and Table 1). An additional six regulators had 5- to 10-fold reductions in opaque-to-white switching; five of these had not previously been linked to switching. We note that many of the newly identified regulators affecting switching rates in either direction (white-to-opaque and/or opaque-to-white) have been previously implicated in the regulation of processes such as carbon or nitrogen utilization, the responses to pH or metals, and filamentation (Table 2). We will return to this topic below.

We note that our screen was carried out in one strain background (SC5314) and under one condition (synthetic complete media supplemented with 2% glucose). Previous studies have indicated that white–opaque switching rates can vary between growth conditions and strain backgrounds (see, for example, Ramírez-Zavala *et al.* 2008, 2013; Huang *et al.* 2009, 2010; and Du *et al.* 2012). As such, our identification of regulators affecting white–opaque switching may be an underestimate since it does not take into account different conditions or different strain backgrounds.

White-to-opaque and opaque-to-white switching rates are not interdependent

Most of the previously described mutants that affect white–opaque switching are locked in one of the two cell types or at least highly biased toward one cell type or the other. Given this initial observation, one might have expected that switching rates in the white-to-opaque and opaque-to-white directions would be inversely correlated. To test this idea, we compared the white-to-opaque and opaque-to-white switching rates for all 53 mutants with altered switching rates (greater than threefold difference compared with the parental strain in at least one direction and switching rates determined for both directions) (Figure 2C and Table S5, comparisons 1–3). Although some deletion mutants did show an inverse correlation (for example, *efg1*, *stp2*, *cup9*, and *fgr15*), such inverse relationships were not the rule, as many of the mutants (for example, *rap1*) affected switching in only one direction. Other mutants (for example, *zcf21* and *asg1*) reduced switching rates in both directions. If we consider all 53 mutants with greater than threefold altered switching frequencies, there was not a strong inverse correlation with switching in the opposite direction (Pearson's r, −0.15; Spearman's rho, −0.21; Table S5, comparison 3). These observations show that the frequency of white-to-opaque and opaque-to-white switching are separable by mutation and that the two rates are not necessarily interdependent. An additional conclusion, based on these observations, is that opaque-to-white switching is not simply the reverse of white-to-opaque switching.

Genome-wide data do not predict regulators of white–opaque switching

Many of the previously known genes that regulate white–opaque switching were initially studied because of differential transcription between the two cell types or the binding of previously established switching regulators to the target gene. Examination of all the genes that, in our screen, showed at least a 10-fold effect on white–opaque switching reveals that neither differential regulation nor regulator binding is a highly accurate predictor of involvement in switching. In fact, fewer than half of the regulators affecting either white-to-opaque or opaque-to-white switching were more than twofold differentially expressed between the two cell types (Table S5, comparison 4, and File S2). Conversely, deletion of <20% of the regulators whose RNA showed a twofold or greater enrichment in one cell type or the other had a >10-fold effect on switching (File S2). We observed a similar poor correlation when examining the previously reported binding [chromatin immunoprecipitation (ChIP)] targets of the eight "core" regulators; only about one-third of the regulators affecting white-to-opaque or opaque-to-white switching at least 10-fold showed binding of the core regulators to their upstream regions and only 25% of regulators bound in white cells and 15% of regulators bound in opaque cells had a >10-fold effect on switching when deleted (Table S5, comparisons 10 and 12, and File S2). Thus, although the genome-wide data sets were historically useful for identifying candidate white–opaque regulators to be tested experimentally, they were not—in retrospect—strongly predictive (Table S5).

Differences in growth rates do not predict white–opaque switching effects

It has been hypothesized that increased white-to-opaque switching could be caused by slow cell growth and division under some conditions, allowing Wor1 to accumulate to critical levels in white cells (Alby and Bennett 2009). We

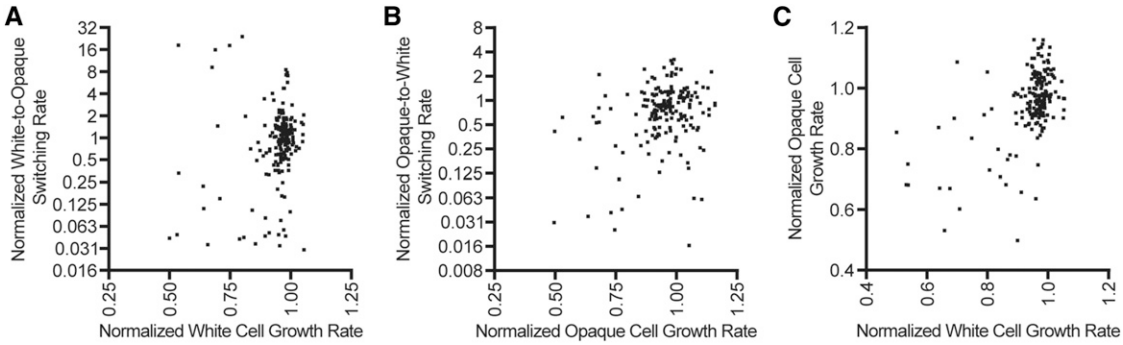

Figure 3 There is no overall correlation between growth rate and switching. (A) Comparison of normalized white-to-opaque switching frequencies and normalized white cell maximum growth rate for 191 strains (Pearson's *r*, −0.29; Spearman's rho, 0.21). (B) Comparison of normalized opaque-to-white switching frequencies and normalized opaque cell maximum growth rate for 187 strains (Pearson's *r*, 0.21; Spearman's rho, 0.21). (C) Comparison of the normalized white cell maximum growth rate and the normalized opaque cell maximum growth rate for 185 strains (Pearson's *r*, 0.54; Spearman's rho, 0.38). Normalized switching rates are plotted on a $\log_2$ scale and normalized maximum growth rates are plotted on a linear scale.

tested this idea broadly by determining growth rates for both the white and opaque versions of the *C. albicans* switching-capable transcription factor mutant library under a standard set of laboratory conditions (SD+aa+Uri at 25°) and comparing these results to switching frequencies. We found that only 5 of the 14 slowest growing white strains exhibited greater than a fivefold increase in white-to-opaque switching. For other slow-growing strains, switching frequencies either decreased or remained at wild-type levels (Figure 3). Furthermore, slow white cell growth was not necessary for increased switching rates as we observed greater than fivefold increases in white-to-opaque switching frequencies in 5 strains with normal growth rates. We conclude from these observations that there is no simple correlation between growth rates and white–opaque switching (Table S5, comparisons 22–31).

We also tested whether the growth rates of white and opaque cells were correlated. A majority of the deletions (~160) had a minor or no effect on the growth rate of either cell type while seven (*hap2*, *hap5*, *hcm1*, *hfl1*, *ino4*, *rca1*, and *stp2*) decreased the growth rate in both cell types. Seven other deletions decreased growth in only the white cell type and 11 decreased growth in only the opaque cell type (Figure 3C, Table 3, and Table S5, comparison 32). We have set a threshold of a 20% reduction in growth rate for these analyses. We note that many of the regulators with cell-type-specific effects are associated with filamentation (Asg1, Ash1, Dpb4, Gln3, and Mac1 in opaque cells) or response to various stresses (Swi4, Rpn4, Cas5, Rap1, and Rfg1 for white cells; Cap1, Gis2, Gln3, and Hap31 for opaque cells), highlighting the broad range of differences between the two cell types.

As was observed with the regulators affecting switching rates, most of the regulators that affect growth (20 of the 25) are not differentially expressed between the two cell types. We do not yet understand the mechanism by which the regulators whose messenger RNA (mRNA) is not differentially expressed have cell-type-specific effects. Possibilities include interactions with other regulators that are expressed in a cell-type-specific manner or some form of cell-type-specific post-transcriptional regulation.

WOR1 transcript levels correlate with altered white-to-opaque switching frequencies in a subset of strains

As previously discussed, Wor1 is often considered the master regulator of white–opaque switching, as it is essential for the formation of the opaque state. Based on Wor1's central role, we hypothesized that changes in *WOR1* transcript levels could account for many of the effects on white-to-opaque switching frequencies observed for the deletion strains. To test this idea, we examined *WOR1* transcript levels by RT-qPCR in eight mutant strains, four with increased, two with reduced, and two with normal white-to-opaque switching rates. Relative to the wild-type white strain, we observed that one mutant strain with an increased switching rate (*lys143*) had sixfold elevated *WOR1* levels in white cells and that one strain with a reduced switching rate (*mig1*) had threefold reduced *WOR1* levels in white cells (Figure S1). Lys143 is known to bind to the *WOR1* promoter (Pérez *et al.* 2014) and our results therefore suggest that Lys143 represses *WOR1*, and that the loss of this repression produces the increase in *WOR1* levels in white cells and consequent elevated white-to-opaque switching. It is not known whether Mig1 directly regulates *WOR1* expression. The other six mutants exhibited no significant changes in *WOR1* transcript levels relative to the wild type. Thus we can conclude that some, but not all, of the altered switching rates correlate with altered *WOR1* levels.

Identification of regulators affecting opaque cell morphology

We have focused on differences in colony morphology between the white and opaque cell types thus far; however, this is not the only morphological difference between the two cell types. The opaque cell type has a distinct morphology relative to the white cell type; opaque cells are more elongated, "fatter," and have a large, easily observed vacuole (Slutsky *et al.* 1987). We

Table 3 List of mutants with 20% or greater effects on growth rate in either white or opaque cells

TFKO number	Name	Normalized white cell growth rate	Normalized opaque cell growth rate
TF074	ASG1	0.895	0.776
TF112	ASH1	0.960	0.636
TF140	CAP1	0.874	0.779
TF033	CAS5	0.700	1.086
TF094	DPB4	0.899	0.498
TF156	EFG1	0.800	1.053
TF045	GAL4	0.789	0.912
TF144	GIS2	0.866	0.764
TF018	GLN3	0.835	0.798
TF087	HAP2	0.658	0.531
TF079	HAP31	0.807	0.729
TF196	HAP41	0.842	0.707
TF194	HAP42	0.861	0.682
TF093	HAP5	0.708	0.602
TF036	HCM1	0.537	0.749
TF103	HFL1	0.532	0.682
TF185	INO2	0.500	0.854
TF081	INO4	0.538	0.681
TF065	MAC1	0.912	0.657
TF125	NRG1	0.633	N/A[a]
TF158	RAP1	0.690	0.900
TF113	RBF1	N/A[b]	0.496
TF058	RCA1	0.642	0.671
TF003	RPN4	0.748	0.834
TF121	SSN6	N/A[b]	0.731
TF162	STP2	0.676	0.670
TF134	SWI4	0.639	0.870
TF024	ZCF21	0.967	0.746

Each value represents the average maximum growth rate of three wells on a given day normalized to the maximum growth rate of the wild-type white or opaque strain on that day. Growth rates of all but one of the strains with a 20% growth defect in white cells and all of the strains with a 20% growth defect in opaque cells were significantly different from wild type (Welch's *t*-test (two tailed) with BH step-up procedure, $\alpha = 0.05$, see File S1 for details).
[a] No opaque isolate.
[b] No white isolate.

screened the opaque version of the deletion library grown under standard laboratory conditions (SD+aa+Uri at 22°) for abnormal cell morphologies using a light microscope, and found 12 strains that exhibited abnormal opaque cell morphologies but normal white cell morphology (Figure 4 and File S2). These abnormalities included shorter, fatter opaque cells, thinner, longer opaque cells, and opaque cells with various "other" irregular appearances. The three regulators whose deletion produces the fatter opaque cell phenotype (Brg1, Yox1, and Ofi1; see Figure 4B) are all upregulated in the opaque cell type, suggesting that the upregulation of these genes contributes to the stereotypical elongated opaque cell morphology. These three regulators do not affect switching rates in either direction when deleted, suggesting that they function downstream of the switching circuit. In contrast, most of the other nine genes implicated in unusual opaque cell morphology are not upregulated in opaque cells.

Many of these 12 regulators needed for normal opaque cell morphology have been previously linked to filamentation (see, for example, Uhl *et al.* 2003 and Du *et al.* 2015). Moreover, the mutants producing the longer cellular morphology also exhibited a wrinkly or fuzzy opaque colony morphology, a phenotype associated with abnormal filamentation. These observations suggest that the opaque cell program may depend, in part, on capturing certain aspects of the filamentation program while preventing other features of it from being expressed.

Examination of the effects of ectopic expression on switching rates

Many of the previously identified regulators of white–opaque switching drive either white-to-opaque or opaque-to-white switching when ectopically expressed. For example, ectopic expression of *CZF1*, *OFI1*, *WOR1*, *WOR3*, or *WOR4* increases white-to-opaque switching, while ectopic expression of *AHR1* or *EFG1* increases opaque-to-white switching (Sonneborn *et al.* 1999; Huang *et al.* 2006; Zordan *et al.* 2006, 2007; Vinces and Kumamoto 2007; Wang *et al.* 2011; Lohse *et al.* 2013; Du *et al.* 2015; Lohse and Johnson 2016). To extend this analysis, we used a doxycycline-inducible system to ectopically express 48 regulators, including many of the transcriptional regulators whose deletion affected switching in one or both directions. Even with a lenient threshold (twofold change, $P < 0.1$), only 12 of these 48 regulators affected switching when ectopically expressed; 8 stimulated white-to-opaque switching (Cap1, Czf1, Fgr15, Flo8, Hap43, Ino4, Rim101, and Zcf21), 3 stimulated opaque-to-white switching (Gal4, Rca1, and Sko1), and 1 affected switching in both directions (Ash1) (Table S4). Six of the 12 regulators identified by ectopic expression also had at least a 10-fold effect on white-to-opaque or opaque-to-white switching when deleted, and an additional 3 had at least a threefold effect (see Table S4 for comparisons to deletion mutant switching rates for all 48 ectopically expressed regulators). These results show that ectopic gene expression does not necessarily produce the opposite effect of a gene deletion, and illustrates the value of screening both gene deletion and gene ectopic expression libraries. These results also reinforce the idea that white-to-opaque and opaque-to-white switching rates are not strictly interdependent.

Pathways and environmental signals that affect switching rates

Examination of the newly identified transcriptional regulators revealed many connections between white–opaque switching and other cellular pathways. For example, deletion of transcription regulators known to affect carbon metabolism had pronounced effects on white–opaque switching. Deletion of *MIG1*, *GAL4*, or *ZCF7* resulted in a 30-fold decrease, a 25-fold decrease, and a 4.7-fold increase, respectively, in white-to-opaque switching frequencies. This observation is consistent with previous observations that glucose levels affect opaque cell stability at elevated temperatures (Lohse *et al.* 2013) and that alternative carbon sources like GlcNAc (Huang *et al.* 2010) affect switching rates. We also noticed that the deletion of a number of white–opaque regulators also affects nitrogen utilization, pH response, response to metals (especially

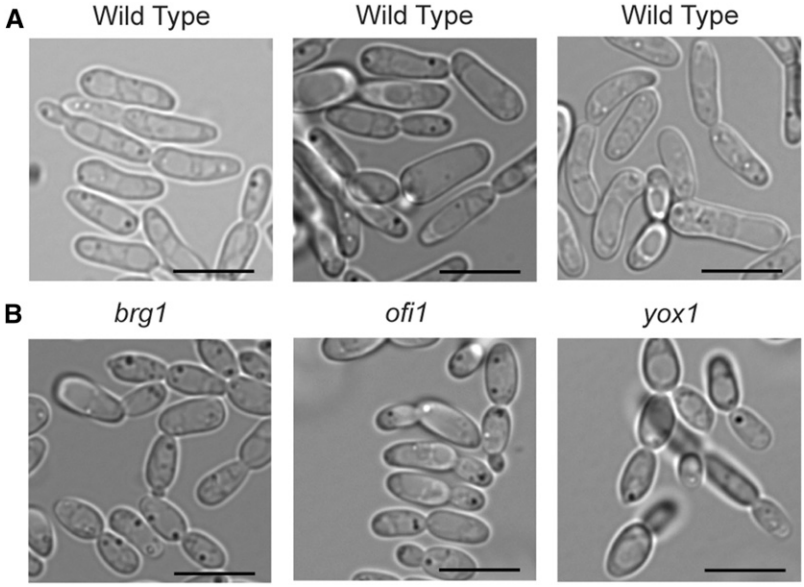

Figure 4 Identification of new regulators of opaque cell morphology. (A) Images of typical wild-type opaque cells. (B) Images of three deletion mutants that result in a shorter, fatter, more oval opaque cell morphology. Bars, 10 μm.

copper), in addition to filamentation (Figure 5 and Table 2). Relationships between some of these processes and switching have previously been noted (Nie *et al.* 2010; Si *et al.* 2013; Sun *et al.* 2015).

We also found examples where deletion of each of several members of a well-defined regulatory complex or pathway produced similar effects on switching. For example, deletion of several members of the CCAAT complex (*HAP2*, *HAP31*, and *HAP5*) reduced white-to-opaque switching at least fivefold (Figure 6A). In addition to roles in filamentation and the responses to copper and iron, the CCAAT complex has been implicated in the regulation of respiration (specifically the electron transport chain) in response to carbon starvation (Johnson *et al.* 2005). Given the effect of *hap2*, *hap31*, and *hap5* on switching, it was surprising that the *hap43* deletion did not have a similar impact, as Hap43 is part of the same complex. However, it has been noted that several of the genes encoding the *C. albicans* CCAAT complex have undergone duplications relative to *Saccharomyces cerevisiae* (Sc*HAP3* to Ca*HAP3* and Ca*HAP31*; Sc*HAP4* to Ca*HAP41*, Ca*HAP42*, and Ca*HAP43*) (Johnson *et al.* 2005) and we hypothesized that only one member of each duplicated group might be important for switching. To test this hypothesis, we constructed deletions for the two paralogs of this complex (*HAP41* and *HAP42*) that were not present in our original deletion library. Consistent with our model, deletion of *HAP41* reduced white-to-opaque switching, while deletion of *HAP42* had little effect (Figure 6A).

Another unanticipated link between white–opaque switching and a regulatory complex came from the deletion of *INO4*, which reduced white-to-opaque switching by a factor of three (Figure 6B). Ino4 is predicted to form a dimer with the regulator Ino2 (Hirsch and Henry 1986; Hoppen *et al.* 2007), which was absent from our original deletion library, and we hypothesized that white-to-opaque switching would also be reduced in an *ino2* deletion. We constructed the *ino2* mutant and, consistent with our model, found that the deletion of *INO2* reduced white-to-opaque switching by a factor of 20 (Figure 6B). The *C. albicans* Ino2 and Ino4 proteins have been predicted to regulate inositol biosynthesis (based on the function of their *S. cerevisiae* orthologs), but, to our knowledge, this has not been tested directly; it has also been suggested that Ino2 and Ino4 regulate ribosomal protein genes (Hoppen *et al.* 2007).

Discussion

White and opaque cells differ in many ways, including their ability to mate, their metabolic preferences, their response to specific environmental signals, and their interactions with the innate immune system. Switching between the two cell types is controlled by a highly interconnected network of transcriptional regulators, and the rate of switching between cell types can be influenced by a wide range of environmental signals. Through quantitative screening of a library of 196 deletion mutants, we have tripled the number of known transcriptional regulators that have large effects (>10-fold) on white-to-opaque and/or opaque-to-white switching rates (Table 1). We also identified a number of additional regulators with more subtle effects on switching, as well as regulators needed specifically by white or opaque cells for their characteristic cell morphology and growth rates. In the paragraphs below, we list the major conclusions derived from this screen.

(1) There is no overall correlation or anticorrelation of forward (white-to-opaque) and backward (opaque-to-white) switching rates. Although a few of the newly identified deletions affect switching in both directions, most (77%, or 41 of 53 regulators with a threefold effect) affect the rate in only one direction. The fact that so many transcription regulator deletion mutants affect switching in only one direction suggests that opaque-to-white switching is not simply the reverse of white-to-opaque switching,

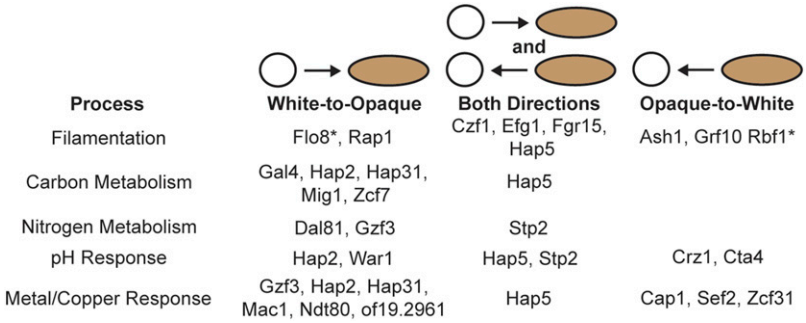

Figure 5 Regulators of selected processes whose deletion affects either white-to-opaque or opaque-to-white switching at least threefold. The direction(s) of each regulator's effect is indicated. It was only possible to screen switching in one direction for regulators marked with *.

and that the forward and backward switching rates are controlled independently. A "unidirectional" switching effect has also been reported for some Mediator complex and chromatin remodeler mutations (Srikantha *et al.* 2001; Hnisz *et al.* 2009; Stevenson and Liu 2013; Zhang *et al.* 2013). These mutations produce global changes in transcription, and it is possible that some of the transcription regulators we have identified exert their effects through these complexes.

(2) There is no simple correlation between cell division rates and switching. Previous studies showed that slow growth could lead to increased white-to-opaque switching under a subset of conditions (Alby and Bennett 2009), but our results indicate that this is not a general rule. For example, many of the slow-growing mutants examined in this study exhibit normal switching rates. Conversely, many mutants exhibiting normal growth rates have altered switching frequencies. Although regulators whose deletion causes slow growth are more likely than chance to also effect white–opaque switching, both increases and decreases in switching frequencies were observed. The results argue strongly against a straightforward causal relationship between slow growth and increased switching.

(3) Although some regulators probably act by controlling levels of Wor1 in white cells, thereby tipping the balance of this master regulator toward the white or opaque cell type, others do not. Thus, white–opaque switching rates can be controlled by pathways that act independently of the expression of *WOR1*.

(4) The specialized properties of opaque cells can be uncoupled from the switching mechanism itself. This conclusion is based on the identification of mutants that affect opaque cell appearance but have no effect on white cell appearance or on switching rates.

(5) No known simple criterion (*e.g.*, differential gene expression between white and opaque cells or binding of genes by previously identified regulators) could have been used *a priori* to identify the majority of the transcriptional regulators whose deletion affects switching. Indeed, the traditional genome-wide "data-mining" approaches appear to have reached the limits of their predictive value as—in retrospect—they would have implicated fewer than half of the newly identified regulators. One reason for this limitation is that most of the newly identified regulators are not themselves differentially expressed between the two cell types. Possible explanations for their cell-type-specific effects include cell-type-specific regulation of translation, changes in cellular localization, and interactions with other cell-type-specific regulators. The important point is that there is no real substitute for the direct screening of mutants.

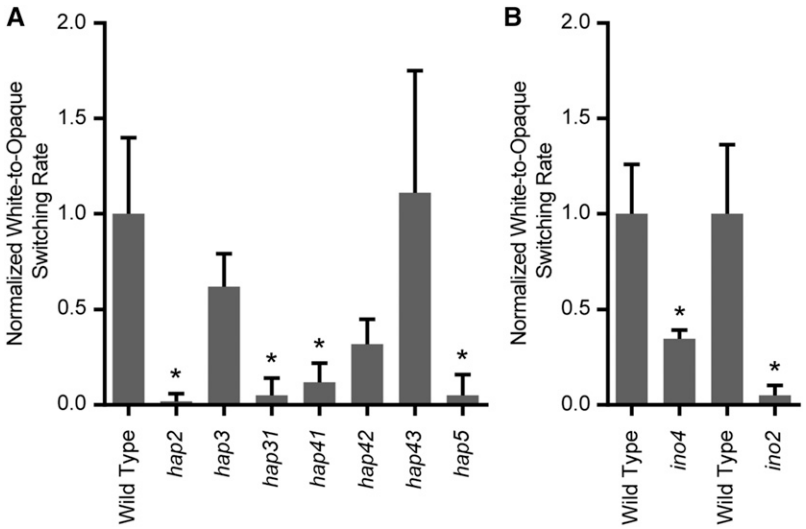

Figure 6 Analysis of regulators that function in specific metabolic complexes or pathways. (A) Effects of deleting various members of the *C. albicans* CCAAT complex on white-to-opaque switching. (B) Deletion of either member of the *C. albicans* Ino2/4 dimer reduces white-to-opaque switching rates. The *ino4* mutant was constructed in the strain background corresponding to the left wild-type sample; the *ino2* mutant was constructed in the strain background corresponding to the right wild-type sample. In both panels, the mean and SD of four (mutant) or five (wild type) independent replicates from the same day are plotted. Data in both panels are normalized to the white-to-opaque switching rates of the matched wild-type control strain from the same day. Strains marked with an * have switching rates that are significantly different relative to their corresponding wild-type strains (Welch's *t*-test, two tailed, $P < 0.01$).

(6) Thirteen percent (26) of the 196 regulators we screened had >10-fold effects on white–opaque switching and an additional 8% (16 more) had more subtle effects (5- to 10-fold) on switching. Although it is difficult to directly compare these numbers to other networks, the number of identified regulators is considerably higher than that observed for other complex circuits, such as *C. albicans* biofilm formation (nine regulators) (Nobile *et al.* 2012; Fox *et al.* 2015). One important difference between white–opaque switching and many other networks is that the white and opaque cell types are stable for many generations, while most networks require the continuous presence of an external signal to remain in one form or the other. This unusual stability of white and opaque cells may require additional circuit complexities, as evidenced by the large number of regulators identified by this screen.

(7) Many of the genes that affected opaque cell growth rates and cellular morphology (without affecting switching or the phenotype of white cells) are also regulators of filamentation, indicating that the opaque cell program may depend in part on repurposing components of the filamentation program. Although this connection has been noted in other studies (Huang *et al.* 2010; Si *et al.* 2013; Du *et al.* 2015), our results establish that several known regulators of filamentous growth are also required for the normal opaque cell morphology.

(8) White-to-opaque and opaque-to-white switching rates are closely tied to diverse metabolic processes. This conclusion is based on the identification of mutants that affect switching that also directly regulate key metabolic processes. For example, the CCAAT complex (Hap2, Hap31, and Hap5), needed for normal white-to-opaque switching, also regulates respiration in response to carbon availability (Johnson *et al.* 2005). We confirmed the connection of the pathway with white–opaque switching by deleting another component of the pathway (*HAP41*) and observing significant effects on switching rates. Identification of the CCAAT complex as a regulator of white-to-opaque switching provides a mechanistic link with the previous observation that genes related to aerobic respiration are upregulated in opaque cells (Lan *et al.* 2002). Furthermore, the CCAAT complex has been linked to peroxisome regulation (Singh *et al.* 2011), potentially tying it to fatty acid β-oxidation, another metabolic process upregulated in opaque cells (Lan *et al.* 2002).

(9) Our screen also revealed other links between switching and metabolism (Figure 5 and Table 2). These include nitrogen utilization (linked to white–opaque switching by the regulators Dal81, Gzf3, and Stp2), pH response (linked by War1 and Stp2), and response to metals (linked by Cap1, Gzf3, Mac1, Sef2, and Zcf31, among others). In addition to establishing these links (some of which have been previously noted by other types of studies), our work provides an entry point—one or more common transcription regulators—to determining the mechanistic bases of these connections.

In summary, through systematic screening, we have identified 19 previously unknown regulators of white–opaque switching in *C. albicans*. The large number of new regulators and their links to cell growth and metabolism establish that white–opaque switching is integrated with many aspects of cellular physiology. This study provides a framework for understanding how the regulation of white–opaque switching is coupled to central metabolic pathways in the cell and for understanding the basis for the metabolic differences between the two cell types.

Acknowledgments

We thank Chiraj Dalal, Naomi Ziv, and Clarissa Nobile for helpful discussions during this project. We thank Ananda Mendoza and Jeanselle Dea for technical assistance. This study was supported by National Institutes of Health (NIH) grants R01-AI049187 (A.D.J.) and R01-AI081704 (R.J.B), and by an Investigator in the Pathogenesis of Infectious Disease Award from the Burroughs Wellcome Fund (R.J.B.). I.V.E. was supported by a Sigma Delta Epsilon fellowship from Graduate Women in Science. E.M. was supported by the Human Frontier Science Program and University of California Institute for Mexico and the United States. J.M. was supported by Deutsche Forschungsgemeinschaft (DFG grant MO 846/5). The content is the sole responsibility of the authors and does not represent the views of the NIH. A.D.J. is a cofounder of BioSynesis, a company developing inhibitors and diagnostics of *C. albicans* biofilm formation and M.B.L. is an employee of BioSynesis; however, there are no conflicts of interest to declare with regards to this manuscript.

Literature Cited

Alby, K., and R. J. Bennett, 2009 Stress-induced phenotypic switching in *Candida albicans*. Mol. Biol. Cell 20: 3178–3191.

Du, H., G. Guan, J. Xie, F. Cottier, Y. Sun *et al.*, 2012 The transcription factor Flo8 mediates CO2 sensing in the human fungal pathogen *Candida albicans*. Mol. Biol. Cell 23: 2692–2701.

Du, H., X. Li, G. Huang, Y. Kang, and L. Zhu, 2015 The zinc-finger transcription factor, Ofi1, regulates white-opaque switching and filamentation in the yeast *Candida albicans*. Acta Biochim. Biophys. Sin. (Shanghai) 47: 335–341.

Fox, E. P., E. S. Cowley, C. J. Nobile, N. Hartooni, D. K. Newman *et al.*, 2014 Anaerobic bacteria grow within *Candida albicans* biofilms and induce biofilm formation in suspension cultures. Curr. Biol. 24: 2411–2416.

Fox, E. P., C. K. Bui, J. E. Nett, N. Hartooni, M. C. Mui *et al.*, 2015 An expanded regulatory network temporally controls *Candida albicans* biofilm formation. Mol. Microbiol. 96: 1226–1239.

Gagneur, J., O. Stegle, C. Zhu, P. Jakob, M. M. Tekkedil *et al.*, 2013 Genotype-environment interactions reveal causal pathways that mediate genetic effects on phenotype. PLoS Genet. 9: e1003803.

Geiger, J., D. Wessels, S. R. Lockhart, and D. R. Soll, 2004 Release of a potent polymorphonuclear leukocyte chemoattractant is regulated by white-opaque switching in *Candida albicans*. Infect. Immun. 72: 667–677.

Hernday, A. D., M. B. Lohse, P. M. Fordyce, C. J. Nobile, J. D. DeRisi *et al.*, 2013 Structure of the transcriptional network controlling white-opaque switching in *Candida albicans*. Mol. Microbiol. 90: 22–35.

Hernday, A. D., M. B. Lohse, C. J. Nobile, L. Noiman, C. N. Laksana *et al.*, 2016 Ssn6 defines a new level of regulation of white-opaque switching in *Candida albicans* and is required for the stochasticity of the switch. MBio 7: e01565-15.

Hirsch, J. P., and S. A. Henry, 1986 Expression of the *Saccharomyces cerevisiae* inositol-1-phosphate synthase (*INO1*) gene is regulated by factors that affect phospholipid synthesis. Mol. Cell. Biol. 6: 3320–3328.

Hnisz, D., T. Schwarzmüller, and K. Kuchler, 2009 Transcriptional loops meet chromatin: a dual-layer network controls white-opaque switching in *Candida albicans*. Mol. Microbiol. 74: 1–15.

Homann, O. R., J. Dea, S. M. Noble, and A. D. Johnson, 2009 A phenotypic profile of the *Candida albicans* regulatory network. PLoS Genet. 5: e1000783.

Hoppen, J., M. Dietz, G. Warsow, R. Rohde, and H. J. Schüller, 2007 Ribosomal protein genes in the yeast *Candida albicans* may be activated by a heterodimeric transcription factor related to Ino2 and Ino4 from *S. cerevisiae*. Mol. Genet. Genomics 278: 317–330.

Huang, G., H. Wang, S. Chou, X. Nie, J. Chen *et al.*, 2006 Bistable expression of *WOR1*, a master regulator of white-opaque switching in *Candida albicans*. Proc. Natl. Acad. Sci. USA 103: 12813–12818.

Huang, G., T. Srikantha, N. Sahni, S. Yi, and D. R. Soll, 2009 CO (2) regulates white-to-opaque switching in *Candida albicans*. Curr. Biol. 19: 330–334.

Huang, G., S. Yi, N. Sahni, K. J. Daniels, T. Srikantha *et al.*, 2010 N-acetylglucosamine induces white to opaque switching, a mating prerequisite in *Candida albicans*. PLoS Pathog. 6: e1000806.

Johnson, A., 2003 The biology of mating in *Candida albicans*. Nat. Rev. Microbiol. 1: 106–116.

Johnson, D. C., K. E. Cano, E. C. Kroger, and D. S. McNabb, 2005 Novel regulatory function for the CCAAT-binding factor in *Candida albicans*. Eukaryot. Cell 4: 1662–1676.

Kvaal, C., S. Lachke, T. Srikantha, K. Daniels, J. McCoy *et al.*, 1999 Misexpression of the opaque-phase-specific gene *PEP1* (*SAP1*) in the white phase of *Candida albicans* confers increased virulence in a mouse model of cutaneous infection. Infect. Immun. 67: 6652–6662.

Kvaal, C. A., T. Srikantha, and D. R. Soll, 1997 Misexpression of the white-phase-specific gene *WH11* in the opaque phase of *Candida albicans* affects switching and virulence. Infect. Immun. 65: 4468–4475.

Lan, C., G. Newport, L. Murillo, T. Jones, S. Scherer *et al.*, 2002 Metabolic specialization associated with phenotypic switching in *Candida albicans*. Proc. Natl. Acad. Sci. USA 99: 14907–14912.

Lin, C. H., S. Kabrawala, E. P. Fox, C. J. Nobile, A. D. Johnson *et al.*, 2013 Genetic control of conventional and pheromone-stimulated biofilm formation in *Candida albicans*. PLoS Pathog. 9: e1003305.

Lohse, M. B., and A. D. Johnson, 2008 Differential phagocytosis of white *vs.* opaque *Candida albicans* by *Drosophila* and mouse phagocytes. PLoS One 3: e1473.

Lohse, M. B., and A. D. Johnson, 2009 White-opaque switching in *Candida albicans*. Curr. Opin. Microbiol. 12: 650–654.

Lohse, M. B., and A. D. Johnson, 2016 Identification and Characterization of Wor4, a New Transcriptional Regulator of White-Opaque Switching. G3 (Bethesda) 6: 721–729.

Lohse, M. B., A. D. Hernday, P. M. Fordyce, L. Noiman, T. R. Sorrells *et al.*, 2013 Identification and characterization of a previously undescribed family of sequence-specific DNA-binding domains. Proc. Natl. Acad. Sci. USA 110: 7660–7665.

Miller, M. G., and A. D. Johnson, 2002 White-opaque switching in *Candida albicans* is controlled by mating-type locus homeodomain proteins and allows efficient mating. Cell 110: 293–302.

Morschhäuser, J., 2010 Regulation of white-opaque switching in *Candida albicans*. Med. Microbiol. Immunol. (Berl.) 199: 165–172.

Nie, X., X. Liu, H. Wang, and J. Chen, 2010 Deletion of *EFG1* promotes *Candida albicans* opaque formation responding to pH via Rim101. Acta Biochim. Biophys. Sin. (Shanghai) 42: 735–744.

Nobile, C. J., E. P. Fox, J. E. Nett, T. R. Sorrells, Q. M. Mitrovich *et al.*, 2012 A recently evolved transcriptional network controls biofilm development in *Candida albicans*. Cell 148: 126–138.

Noble, S. M., and A. D. Johnson, 2005 Strains and strategies for large-scale gene deletion studies of the diploid human fungal pathogen *Candida albicans*. Eukaryot. Cell 4: 298–309.

Noble, S. M., S. French, L. A. Kohn, V. Chen, and A. D. Johnson, 2010 Systematic screens of a *Candida albicans* homozygous deletion library decouple morphogenetic switching and pathogenicity. Nat. Genet. 42: 590–598.

Park, Y., and J. Morschhäuser, 2005 Tetracycline-inducible gene expression and gene deletion in *Candida albicans*. Eukaryot. Cell 4: 1328–1342.

Pérez, J. C., P. M. Fordyce, M. B. Lohse, V. Hanson-Smith, J. D. DeRisi *et al.*, 2014 How duplicated transcription regulators can diversify to govern the expression of nonoverlapping sets of genes. Genes Dev. 28: 1272–1277.

Ramírez-Zavala, B., O. Reuss, Y. N. Park, K. Ohlsen, and J. Morschhäuser, 2008 Environmental induction of white-opaque switching in *Candida albicans*. PLoS Pathog. 4: e1000089.

Ramírez-Zavala, B., M. Weyler, T. Gildor, C. Schmauch, D. Kornitzer *et al.*, 2013 Activation of the Cph1-dependent MAP kinase signaling pathway induces white-opaque switching in *Candida albicans*. PLoS Pathog. 9: e1003696.

Rikkerink, E. H., B. B. Magee, and P. T. Magee, 1988 Opaque-white phenotype transition: a programmed morphological transition in *Candida albicans*. J. Bacteriol. 170: 895–899.

Sasse, C., M. Hasenberg, M. Weyler, M. Gunzer, and J. Morschhäuser, 2013 White-opaque switching of *Candida albicans* allows immune evasion in an environment-dependent fashion. Eukaryot. Cell 12: 50–58.

Si, H., A. D. Hernday, M. P. Hirakawa, A. D. Johnson, and R. J. Bennett, 2013 *Candida albicans* white and opaque cells undergo distinct programs of filamentous growth. PLoS Pathog. 9: e1003210.

Singh, R. P., H. K. Prasad, I. Sinha, N. Agarwal, and K. Natarajan, 2011 Cap2-HAP complex is a critical transcriptional regulator that has dual but contrasting roles in regulation of iron homeostasis in *Candida albicans*. J. Biol. Chem. 286: 25154–25170.

Slutsky, B., M. Staebell, J. Anderson, L. Risen, M. Pfaller *et al.*, 1987 "White-opaque transition": a second high-frequency switching system in *Candida albicans*. J. Bacteriol. 169: 189–197.

Soll, D. R., 2009 Why does *Candida albicans* switch? FEMS Yeast Res. 9: 973–989.

Soll, D. R., B. Morrow, and T. Srikantha, 1993 High-frequency phenotypic switching in *Candida albicans*. Trends Genet. 9: 61–65.

Sonneborn, A., B. Tebarth, and J. F. Ernst, 1999 Control of white-opaque phenotypic switching in *Candida albicans* by the Efg1p morphogenetic regulator. Infect. Immun. 67: 4655–4660.

Srikantha, T., L. K. Tsai, K. Daniels, and D. R. Soll, 2000 *EFG1* null mutants of *Candida albicans* switch but cannot express the com-

plete phenotype of white-phase budding cells. J. Bacteriol. 182: 1580–1591.

Srikantha, T., L. Tsai, K. Daniels, A. J. Klar, and D. R. Soll, 2001 The histone deacetylase genes *HDA1* and *RPD3* play distinct roles in regulation of high-frequency phenotypic switching in *Candida albicans*. J. Bacteriol. 183: 4614–4625.

Srikantha, T., A. R. Borneman, K. J. Daniels, C. Pujol, W. Wu *et al.*, 2006 *TOS9* regulates white-opaque switching in *Candida albicans*. Eukaryot. Cell 5: 1674–1687.

Sriram, K., S. Soliman, and F. Fages, 2009 Dynamics of the interlocked positive feedback loops explaining the robust epigenetic switching in *Candida albicans*. J. Theor. Biol. 258: 71–88.

Stevenson, J. S., and H. Liu, 2013 Nucleosome assembly factors CAF-1 and HIR modulate epigenetic switching frequencies in an H3K56 acetylation-associated manner in *Candida albicans*. Eukaryot. Cell 12: 591–603.

Stoldt, V. R., A. Sonneborn, C. E. Leuker, and J. F. Ernst, 1997 Efg1p, an essential regulator of morphogenesis of the human pathogen *Candida albicans*, is a member of a conserved class of bHLH proteins regulating morphogenetic processes in fungi. EMBO J. 16: 1919–1982.

Sun, Y., C. Cao, W. Jia, L. Tao, G. Guan *et al.*, 2015 pH Regulates White-Opaque Switching and Sexual Mating in *Candida albicans*. Eukaryot. Cell 14: 1127–1134.

Tuch, B. B., Q. M. Mitrovich, O. R. Homann, A. D. Hernday, C. K. Monighetti *et al.*, 2010 The transcriptomes of two heritable cell types illuminate the circuit governing their differentiation. PLoS Genet. 6: e1001070.

Uhl, M. A., M. Biery, N. Craig, and A. D. Johnson, 2003 Haploinsufficiency-based large-scale forward genetic analysis of filamentous growth in the diploid human fungal pathogen *C. albicans*. EMBO J. 22: 2668–2678.

Vinces, M., and C. A. Kumamoto, 2007 The morphogenetic regulator Czf1p is a DNA-binding protein that regulates white opaque switching in *Candida albicans*. Microbiology 153: 2877–2884.

Wang, H., W. Song, G. Huang, Z. Zhou, Y. Ding *et al.*, 2011 *Candida albicans* Zcf37, a zinc finger protein, is required for stabilization of the white state. FEBS Lett. 585: 797–802.

Zhang, A., Z. Liu, and L. C. Myers, 2013 Differential regulation of white-opaque switching by individual subunits of *Candida albicans* mediator. Eukaryot. Cell 12: 1293–1304.

Zordan, R. E., D. J. Galgoczy, and A. D. Johnson, 2006 Epigenetic properties of white-opaque switching in *Candida albicans* are based on a self-sustaining transcriptional feedback loop. Proc. Natl. Acad. Sci. USA 103: 12807–12812.

Zordan, R., M. Miller, D. Galgoczy, B. Tuch, and A. Johnson, 2007 Interlocking transcriptional feedback loops control white-opaque switching in *Candida albicans*. PLoS Biol. 5: e256.

Communicating editor: A. Hinnebusch

GENETICS

Supporting Information
www.genetics.org/lookup/suppl/doi:10.1534/genetics.116.190645/-/DC1

Systematic Genetic Screen for Transcriptional Regulators of the *Candida albicans* White-Opaque Switch

Matthew B. Lohse, Iuliana V. Ene, Veronica B. Craik, Aaron D. Hernday, Eugenio Mancera, Joachim Morschhäuser, Richard J. Bennett, and Alexander D. Johnson

DOI: 10.1534/genetics.116.190645

Figure S1: *WOR1* transcript levels do not necessarily correlate with white-to-opaque switching rates. *WOR1* transcript levels determined by qPCR and white-to-opaque switching rates for eight deletion mutations as well as heterozygous and homozygous *wor1* deletions are shown. Both values are normalized to those of the wild type white strain. Normalized switching rates are plotted on a $\log_2$ scale, normalized *WOR1* transcript levels are plotted on a linear scale. (.tif, 716 KB)

Available for download as a .tif file as:
http://www.genetics.org/lookup/suppl/doi:10.1534/genetics.116.190645/-/DC1/FigureS1.tif

Table S1: List of oligonucleotides used in this study. (.xlsx, 12 KB)

Available for download as a .xlsx file as:

http://www.genetics.org/lookup/suppl/doi:10.1534/genetics.116.190645/-/DC1/TableS1.xlsx

Table S2: List of plasmids used in this study. (.xlsx, 12 KB)

Available for download as a .xlsx file as:

http://www.genetics.org/lookup/suppl/doi:10.1534/genetics.116.190645/-/DC1/TableS2.xlsx

Table S3: List of strains used in this study. (.xlsx, 22 KB)

Available for download as a .xlsx file as:

http://www.genetics.org/lookup/suppl/doi:10.1534/genetics.116.190645/-/DC1/TableS3.xlsx

Table S4: Ectopic Expression Screen. White-to-opaque and opaque-to-white switching frequencies for ectopic expression (+dox) of 48 regulators and two controls (Wor1, Efg1) relative to the un-induced basal switching frequency (-dox). Ectopic expression of 12 of the 48 regulators as well as the Wor1 control had at least a two-fold effect on switching in at least one direction that was statistically significant ($p<0.1$ for +dox versus –dox, Paired T-test, two-tailed). Normalized white-to-opaque and opaque-to-white switching frequencies for the related deletion strains are also presented. (.xlsx, 15 KB)

Available for download as a .xlsx file as:
http://www.genetics.org/lookup/suppl/doi:10.1534/genetics.116.190645/-/DC1/TableS4.xlsx

Table S5: Analysis of correlation and observed versus expected overlap in switching frequencies and other metrics. For two given metrics ("Condition A" and "Condition B"), we report the number of mutants that had data for each ("Total Regulator #"), the number of mutants meeting each individual criteria ("Condition A Regulator #" and "Condition B Regulator #"), and the number of mutants meeting both criteria ("A and B Overlap Regulator #"). We then evaluate how effective Condition B is at predicting Condition A by calculating how many regulators are explained by B ("Fraction of A Explained By B", equal to "A and B Overlap Regulator #" divided by "Condition A Regulator #") and the fraction we would expect by chance based on the prevalence of regulators meeting condition B for all regulators considered ("Fraction of A Expected", equal to "Condition B Regulator #" divided by "Total Regulator #"). We then calculate the reverse, how well Condition A predicts Condition B by performing the equivalent analyses for regulator B. The enrichment of B predicting A, which is also the enrichment of A predicting B, relative to that expected by chance ("Enrichment Relative to Full Regulator Set"), is equal to the "Fraction of A Explained By B" divided by the "Fraction of A Expected" which is equivalent to the "Fraction of B Explained By A" divided by the "Fraction of B Expected." We then determined if this enrichment is statistically significant using the Hypergeometric Distribution (Sample Success, "A and B Overlap Regulator #"; Sample Size, "Condition A Regulator #"; Population Success, "Condition B Regulator #"; Population Size, "Total Regulator #"). We calculated correlation coefficients (both Pearson's r and Spearman's rho) using GraphPad Prism 6. Due to the limitation of each comparison to regulators that had data for both conditions, many comparisons use fewer regulators than are reported for the full data sets. See File S1 for details of regulators missing from specific comparisons as well as descriptions of the individual comparisons. Transcriptional enrichment data (Tuch *et al.* 2010) and ChIP-chip and ChIP-seq binding data (Zordan *et al.* 2007; Hernday *et al.* 2013, 2016; Lohse *et al.* 2013; Lohse and Johnson 2016) have been previously reported. These calculations are described in detail in File S1. (.xlsx, 12 KB)

Available for download as a .xlsx file as:

http://www.genetics.org/lookup/suppl/doi:10.1534/genetics.116.190645/-/DC1/TableS5.xlsx

File S1

Systematic genetic screen for transcriptional regulators of the *Candida albicans* white-opaque switch

Matthew B. Lohse[a,1], Iuliana V. Ene[b], Veronica B. Craik[a], Aaron D. Hernday[c], Eugenio Mancera[a], Joachim Morschhäuser[d], Richard J. Bennett[b], and Alexander D. Johnson[a,e,2]

[a]Department of Microbiology and Immunology, University of California, San Francisco, San Francisco, CA 94158, USA

[b]Department of Molecular Microbiology and Immunology, Brown University, Providence, RI 02912, USA.

[c]Department of Molecular and Cell Biology, University of California, Merced, Merced, CA 95343, USA

[d]Institut für Molekulare Infektionsbiologie, Universität Würzburg, D-97080, Würzburg, Germany

[e]Department of Biochemistry and Biophysics, University of California, San Francisco, San Francisco, CA 94158, USA

[1]Present address: Department of Biology, BioSynesis, Inc., San Francisco, USA

[2]Address correspondence to: Alexander D. Johnson (ajohnson@cgl.ucsf.edu)

Supplemental Materials and Methods

Details of strains excluded from some analyses

We have assigned TF mutant numbers for 197 strains. As noted in the Materials and Methods, we could not convert one of these (TF184 (*gcn4*)) to a switching capable background due to a lack of suitable markers. As such, the white-opaque switching capable library consists of 196 strains (TF1-TF183, TF185-197). It was not possible to obtain a homozygous deletion for one of the remaining strains, TF182 (*CBF1*), so in this case the heterozygous deletion (*CBF1*/*cbf1*) was tested. This strain did not have a three-fold effect on switching in either direction or exhibit growth rate defects in either cell type, so its exclusion would not have changed the overall trends.

Three mutant strains exhibited phenotypes that limited our ability to gather information on them. The hyperfilamentation of TF117 (*tup1*) and TF125 (*nrg1*) and the septation defects of TF59 (*ace2*) prevented the identification of opaque sectors, if any existed. As such, we could not determine the white-to-opaque switching rate or isolate opaque colonies for these strains. We have included the "switching capable" versions of these strains in the 196 member library, but could not evaluate them in many of the assays (details below).

Several other mutants have limited data due to the inability to isolate cells of a given cell type. Both the TF113 (*rbf1*) and TF121 (*ssn6*) mutants appear heavily biased to or even locked in the opaque cell type, as such it was not possible to determine white-to-opaque switching rates for them. We were unable to isolate opaque cells for TF56 (*wor2*), TF175 (*flo8*), TF176 (*wor1*), and TF181 (*wor4*); as such we could not determine opaque-to-white switching rates for these strains. The TF137 (*bcr1*) mutant is hyperfilamentous in the opaque cell type and the hyperfilamentous

colony morphology prevented us from performing opaque-to-white switching assays or opaque cell growth rate assays.

We consider TF56 (*wor2*), TF104 (*czf1*), TF121 (*ssn6*), TF132 (*ahr1*), TF156 (*efg1*), TF170 (*wor3*), TF176 (*wor1*), and TF181 (*wor4*) to be the previously known "core" regulatory circuit. We include TF38 (*ofi1*), TF161 (*lys143*), and TF175 (*flo8*) in the list of previously known regulators of white-opaque switching when determining the number of "new" regulators of switching.

Overview of enrichment calculations

The numbers used to perform the enrichment calculations described below are also included in Table S5. Each of the specific comparisons in Table S5 have been assigned a "Comparison Number" that is referred to in the text below. In Table S5, for two given metrics ("Condition A" and "Condition B"), we report the number of mutants that had data for each ("Total Regulator #"), the number of mutants meeting each individual criteria ("Condition A Regulator #" and "Condition B Regulator #"), and the number of mutants meeting both criteria ("A and B Overlap Regulator #"). We then evaluate how effective Condition B is at predicting Condition A by calculating how many regulators are explained by B ("Fraction of A Explained By B", equal to "A and B Overlap Regulator #" divided by "Condition A Regulator #") and the fraction we would expect by chance based on the prevalence of regulators meeting condition B for all regulators considered ("Fraction of A Expected", equal to "Condition B Regulator #" divided by "Total Regulator #"). We then calculate the reverse, how well Condition A predicts Condition B, by performing the equivalent analyses for regulator B. The enrichment of B predicting A relative to that expected by chance ("Enrichment Relative to Full Regulator Set"), is

equal to the "Fraction of A Explained By B" divided by the "Fraction of A Expected" which is equivalent to the "Fraction of B Explained By A" divided by the "Fraction of B Expected" for the enrichment of A predicting B. We then determined if the difference from that expected by chance is statistically significant using the Hypergeometric Distribution (Sample Success, "A and B Overlap Regulator #"; Sample Size, "Condition A Regulator #"; Population Success, "Condition B Regulator #"; Population Size, "Total Regulator #").

We now consider the calculations for Comparison 1 from Table S5 as an example. This comparison is between the mutants with a 10-fold effect on white-to-opaque switching (Set A) and those with a 10-fold effect on opaque-to-white switching (Set B). This comparison uses the set of 186 mutants for which there are both white-to-opaque and opaque-to-white switching rates, the basis for which is discussed below. In this set of 186 mutants, there are 16 mutants with a 10-fold effect on white-to-opaque switching and seven mutants with a 10-fold effect on opaque-to-white switching; three of these mutants affect switching in both the white-to-opaque and opaque-to-white directions. The overlap of Set A and B is 19% of Set A (3/16) while we would have expected 4% by chance (7/186) assuming a random distribution of the two data sets. This represents a 5.0-fold enrichment ((3/16) / (7/186)) over what would have been expected by chance. Likewise, the overlap of set B and A is 43% of set B (3/7) while we would have expected 9% by chance (16/186). We then evaluate if this is significant using the Hypergeometric Distribution (Sample Pass, 3; Sample Size, 16; Population Pass, 7; Population Size, 186) which gives p=1.38e-2. For the analyses presented below, we set the significance threshold for the Hypergeometric Distribution at p<1e-2, as such p=1.38e-2 would not be significant. When possible, we also determine Pearson's correlation coefficient r (which assumes Gaussian distribution of the data) and Spearman's rank correlation coefficient rho (which does

not assume Gaussian distribution of the data) in order to evaluate the correlation between datasets.

Statistical Analysis of Switching Screen

In order to evaluate the relevance of the switching thresholds used in this study (mutants with 10-, five-, or three-fold changes in white-to-opaque or opaque-to-white switching rates), we performed the following statistical analysis (the results of which are included in File S2) to determine if each mutant's switching rate was significantly different than the wild type switching rate. We used the two-tailed Welch's t-test (also called the unequal variances t-test) for each mutant in both the white-to-opaque and opaque-to-white directions, comparing the switching rates for the individual mutant plates (usually six plates) to the switching rates for the individual plates from the five wild type controls from the same day (usually 30 plates). When no switching events were detected on a given plate, we set the switching frequency of that plate to 1 / (number of colonies counted) for the purposes of this analysis. Although this may result in the underestimation of the significance of some mutants (specifically those with reduced switching rates), we wanted to account for differences in the number of colonies counted on different plates. (In other words, acknowledging the difference between no switching events in 200 colonies and no switching events in only 50 colonies). The raw p-values generated are included in File S2, columns U and X.

As we were evaluating 191 strains for the white-to-opaque switching assays and 188 strains for the opaque-to-white switching assays, it was then necessary to correct the raw p-values for multiple comparisons in order to control for Type I errors (false positives). We used the Benjamini-Hochberg procedure (BH step-up procedure) with $\alpha = 0.05$ to correct for multiple

comparisons, with m set to 191 (white-to-opaque) or 188 (opaque-to-white). The results of this statistical analysis are discussed below and are indicated in File S2, columns V and Y.

Statistical Analysis of Growth Rate Assays

In order to evaluate the relevance of the growth rate threshold used in this study (mutants with 20% reductions in white and/or opaque cell growth rates), we performed the following statistical analysis to determine if each mutant's growth rate was significantly different than the wild type growth rate. We used the two-tailed Welch's t-test (also called the unequal variances t-test) for each mutant, comparing the growth rates for the individual mutant wells (usually three) to the growth rates for the individual wild type control wells from the same day (usually three). We used the maximum growth rates (prior to normalization) for these analyses. The raw p-values generated are included in File S2, columns AA and AD. As we were evaluating white cell growth rates for 194 strains and opaque cell growth rates for 187 strains, we corrected the raw p-values for multiple comparisons in order to control for Type I errors (false positives). We used the Benjamini-Hochberg procedure (BH step-up procedure) with $\alpha = 0.05$ to correct for multiple comparisons, with m set to 194 (white cells) or 187 (opaque cells). The results of this statistical analysis are discussed below and are indicated in File S2, columns AB and AE.

CCAAT and Ino2/4 dimer switching assays

The CCAAT and Ino2/4 dimer switching assays from Figure 6 were performed as follows. Two to three white colonies, without visible opaque sectors, were resuspended in water, diluted, plated on SD+aa+Uri, and allowed to grow for one week at room temperature (approximately 22º). We performed five independent replicates for wild type and four

independent replicates for each mutant, all on the same day. As the *ino2* and *ino4* mutants were constructed in different backgrounds, we determined the switching rates for the wild type strain corresponding to each background. Plates were scored using the same criteria described for the initial screen. We determined the mean and standard deviation for the four (mutant) or five (wild type) replicates and normalized to the mean wild type switching rate. Differences in switching rates were evaluated using Welch's t-test (two-tailed).

Supplemental Results

White-to-opaque switching effects

As noted above, we could not determine white-to-opaque switching rates for TF59 (*ace2*), TF113 (*rbf1*), TF117 (*tup1*), TF121 (*ssn6*), and TF125 (*nrg1*). TF113 (*rbf1*) and TF121 (*ssn6*) could reasonably be assumed to have very high white-to-opaque switching rates, however they are not included in the counts below. We were able to determine white-to-opaque switching rates for 191 strains and these data are used in Figures 2A and 3A as well as Comparisons 6-7, 14-15, 18-19, and 22-24 in Table S5.

Twenty of the 191 mutants had at least 10-fold effects on white-to-opaque switching (four increased rates, 16 decreased rates). Removing the six known regulators (TF56 (*wor2*), TF104 (*czf1*), TF156 (*efg1*), TF175 (*flo8*), TF176 (*wor1*), and TF181 (*wor4*)) from this set leaves 14 "new" regulators (three increased rates, 11 decreased rates). An additional 11 regulators had five- to 10-fold effects (six increased rates, five decreased rates). Removing the one known regulator (TF161 (*lys143*)) leaves 10 regulators (five increased rates, five decreased rates). This gives us a total of 31 mutants with at least five-fold effects (10 increased rates, 21 decreased rates) of which seven were previously known. Going to an even more relaxed three-fold cutoff, we find an additional 11 mutants (five increased rates, six decreased rates), none of which were known. This gives us a total of 42 mutants with at least three-fold effects on white-to-opaque switching rates (15 increased rates, 27 decreased rates) of which seven were previously known.

Opaque-to-white switching effects

As noted above, we could not determine opaque-to-white switching rates for TF56 (*wor2*), TF59 (*ace2*), TF117 (*tup1*), TF125 (*nrg1*), TF137 (*bcr1*), TF175 (*flo8*), TF176 (*wor1*),

and TF181 (*wor4*). We determined opaque-to-white switching rates for 188 mutants; these 188 mutants are used in Figure 2B as well as Comparisons 8-9, 16-17, and 20-21 in Table S5.

Nine of the 188 mutants had at least 10-fold effects on opaque-to-white switching (all decreasing rates). Removing the three known regulators (TF104 (*czf1*), TF121 (*ssn6*), and TF156 (*efg1*)) leaves six new regulators (all decreasing rates). An additional six regulators had five- to 10-fold effects (all decreasing rates). Removing the one known regulator (TF132 (*ahr1*)) leaves five new regulators (all decreasing rates). This gives us a total of 15 mutants with at least five-fold effects on opaque-to-white switching (all decreasing rates) of which four were previously known. Going to an even more relaxed three-fold cutoff, we find an additional 14 mutants affecting opaque-to-white switching (three increased rates, 11 decreased rates). Removing the one known regulator (TF170 (*wor3*)) leaves 13 new regulators (three increased rates, 10 decreased rates). This gives us a total of 29 mutants with at least three-fold effects on opaque-to-white switching (three increased rates, 26 decreased rates) of which five were previously known.

Statistical Analysis of the Switching Screens

As discussed above, we used Welch's t-test (two-tailed) to compare the switching rates for the individual mutant plates (usually six plates) to the switching rates for the individual plates from the five wild type controls from the same day (usually 30 plates). Looking at the raw p-values (that is without correcting for multiple comparisons), we note that 38 of the 42 mutants with at least three-fold effects on white-to-opaque switching have p-values of less than 0.001. Twenty-six of the 27 mutants with decreased switching rates had a p-value of less than 0.001 and all had a p-value of less than 0.01. Twelve of the 15 mutants with increased switching rates had a p-value of less than 0.001 and all had a p-value of less than 0.01. Looking at the subset of these

mutants with a five-fold effect on white-to-opaque switching, eight of the 10 mutants with increased switching and all 21 mutants with decreased switching had a p-value of less than 0.001. All 20 mutants with at least a 10-fold effect on white-to-opaque switching had a p-value of less than 0.001. Of the 29 mutants with at least three-fold effects on opaque-to-white switching rates, 28 have p-values of less than 0.001. Two of the three mutants with increased switching rates had a p-value of less than 0.001 and all had a p-value of less than 0.01. All of the 26 mutants with decreased switching rates had a p-value of less than 0.001. Looking at the subset of mutants with five- or 10-fold effects on opaque-to-white switching, all had a p-value of less than 0.001. The raw p-values generated from this analysis are included in File S2 in columns U and X.

Due to the large number of comparisons made (191 for white-to-opaque and 188 for opaque-to-white), it is necessary to correct for the multiple comparisons. To do this, we performed the Benjamini-Hochberg procedure (BH step-up procedure). Using this test, with $\alpha = 0.05$, we find that there are 71 mutants with a significant difference in white-to-opaque switching rates and 86 mutants with a significant difference in opaque-to-white switching rates. These mutants include all of the regulators with three-fold or greater effects on switching in either direction (42 white-to-opaque, 29 opaque-to-white) as well as the smaller subset of mutants with five- or 10-fold effects on switching. We have indicated the mutants that were significant at the $\alpha = 0.05$ threshold for both switching assays in File S2, columns V and Y.

Comparing white-to-opaque and opaque-to-white switching rates

If we consider white-to-opaque and opaque-to-white switching data for mutants with switching rates in at least one direction (regardless of whether they exhibit increased or

decreased switching and without limiting the comparisons to only mutants with switching rates in both directions), we are considering a set of 193 mutants (used in Table S5 Comparisons 4-5, 9-12). This set excludes TF59 (*ace2*), TF117 (*tup1*), and TF125 (*nrg1*).

Of the 193 mutants, 26 have at least a 10-fold effect on switching in one direction (20 affect white-to-opaque switching, nine affect opaque-to-white switching, three of these affect both rates). Seven of these 26 were previously known (TF56 (*wor2*), TF104 (*czf1*), TF121 (*ssn6*), TF156 (*efg1*), TF175 (*flo8*), TF176 (*wor1*), and TF181 (*wor4*)), leaving 19 new regulators of switching (14 affect white-to-opaque switching, six affect opaque-to-white switching, one of these affects both rates). There are 42 mutants with at least a five-fold effect in one direction (31 affect white-to-opaque switching, 15 affect opaque-to-white switching, four of these affect both rates). Nine of the 42 mutants were previously known ((TF56 (*wor2*), TF104 (*czf1*), TF121 (*ssn6*), TF132 (*ahr1*), TF156 (*efg1*), TF161 (*lys143*), TF175 (*flo8*), TF176 (*wor1*), and TF181 (*wor4*)), leaving 33 new regulators (24 affect white-to-opaque switching, 11 affect opaque-to-white switching, two of these affect both rates). There are 59 mutants with at least a three-fold effect on switching in one direction (42 affect white-to-opaque switching, 29 affect opaque-to-white switching, 12 of these affect both rates). Ten of the 59 have been previously reported ((TF56 (*wor2*), TF104 (*czf1*), TF121 (*ssn6*), TF132 (*ahr1*), TF156 (*efg1*), TF161 (*lys143*), TF170 (*wor3*), TF175 (*flo8*), TF176 (*wor1*), and TF181 (*wor4*)), leaving 49 new regulators (35 affect white-to-opaque switching, 24 affect opaque-to-white switching, 10 of these affect both rates).

If we consider only switching data from strains with switching rates in both directions (that is both white-to-opaque and opaque-to-white rates, unlike the previous comparison where one of these rates was sufficient for inclusion), we exclude 10 strains and are thus considering a

set of 186 mutants. As before, this set excludes TF59 (*ace2*), TF117 (*tup1*), and TF125 (*nrg1*). It also excludes TF113 (*rbf1*) and TF121 (*ssn6*) due to a lack of white-to-opaque switching and TF56 (*wor2*), TF175 (*flo8*), TF176 (*wor1*), and TF181 (*wor4*) due to a lack of opaque-to-white switching. TF137 (*bcr1*) was excluded due to opaque hyperfilamentation issues. The remaining 186 mutants are used in Figure 2C as well as Comparisons 1-2 in Table S5. We note that the requirement for switching in both directions excludes some of the strongest effects on switching (i.e. the *wor1* and *ssn6* mutants), as such this may bias the results.

Of the 186 mutants, 20 have at least a 10-fold effect on switching in one direction (16 affect white-to-opaque switching, seven affect opaque-to-white switching, three affect both rates). Moving to a five-fold effect, 36 mutants have an effect (27 affect white-to-opaque switching, 13 affect opaque-to-white switching, four affect both rates). Looking at three-fold effects (the comparison used in the text), there are 53 mutants (38 affect white-to-opaque switching, 27 affect opaque-to-white switching, 12 affect both rates). The subset of 53 mutants with three-fold effects in at least one direction is used in Comparison 3 in Table S5.

We now consider whether one data set (i.e. mutants with a 10-fold effect on white-to-opaque switching rates) does better at predicting members of the other data set (i.e. mutants with a 10-fold effect on opaque-to-white switching rates) than would be expected by chance (based on the fraction of regulators meeting the conditions out of all regulators considered). Considering mutants with 10-fold effects on switching (Table S5 Comparison 1), we observe that mutants with a 10-fold effect in one direction are 5.0-fold more likely to predict mutants with a 10-fold effect in the other direction than would expected by chance. This enrichment is not significant as evaluated by the Hypergeometic Distrubution (p=1.38e-2). Using a 10-fold threshold roughly 60% of mutants affecting opaque-to-white switching and 80% of mutants affecting white-to-

opaque switching would have been missed if we considered only mutations affecting the opposite direction. Considering mutants with three-fold effects on switching (Table S5 Comparison 2), we observe that mutants with a three-fold effect in one direction are 2.2-fold more likely to predict mutants with a three-fold effect in the other direction than would have been expected by chance. This enrichment is significant (p=1.49e-3), however, even at this relaxed threshold roughly 55% of mutants affecting opaque-to-white switching and 70% of mutants affecting white-to-opaque switching would have been missed if considering only mutations affecting the opposite direction. The Pearson correlation coefficient (r, -0.15) and the Spearman rank correlation coefficient (rho, -0.04) suggest that there is not a strong correlation between these two data sets.

As a variation on this comparison, we now consider whether one data set (i.e. mutants with a 3-fold effect on white-to-opaque switching rates) does better at predicting members of the other data set (i.e. mutants with a 3-fold effect on opaque-to-white switching rates) than would be expected by chance when considering only the regulators that affected switching rates in at least one cell type (and that had switching rates in both directions) (Table S5 Comparison 3). As noted above, there are 53 mutants that satisfy this criteria (38 affect white-to-opaque switching, 27 affect opaque-to-white switching, 12 affect both rates). Considering only these 53 regulators (rather than the full set of 186 discussed in the previous paragraph), we observe that mutants with a three-fold effect in one direction are actually worse at predicting regulators with a three-fold effect on the other direction that would be expected by chance (0.62-fold that expected by chance). As with the larger set of 186 regulators, the Pearson correlation coefficient (r, -0.15) and the Spearman rank correlation coefficient (rho, -0.21) suggest that there is not a strong correlation between these two data sets.

Comparisons between switching rates and differential transcription of regulators between cell types.

We now consider comparisons between switching rates and differential expression levels. The comparison in the main text (Table S5 Comparison 4) uses the list of 193 mutants with white-to-opaque and opaque-to-white switching data in at least one direction (in other words, without limiting the comparisons to just those strains with switching rates in both directions and not separating out increases and decreases in switching rates). This set excludes TF59 (*ace2*), TF117 (*tup1*), and TF125 (*nrg1*). We use two-fold differential expression between the white and opaque cell types from previously published RNAseq experiments (Tuch *et al.* 2010) as a threshold.

There are 26 (out of 193) regulators that have at least a 10-fold effect on switching in one direction. Ten of these (38%) are at least two-fold differentially expressed between white and opaque cells. This represents 18% of the 56 regulators (10/56) that are differentially expressed two-fold between the two cell types, a 1.3-fold improvement on what would have been expected by chance, and is not significant (9.33e-2). With these thresholds, a prediction based on differential regulation misses 62% of the regulators affecting switching rates (Table S5 Comparison 4). Considering the 59 regulators with three-fold effects on switching, 32% (19/59) are differentially regulated at least two-fold between cell types and this represents 34% (19/56) of the differentially expressed regulators. This is only a 1.1-fold improvement relative to that expected by chance, is not significant (1.09e-1), and would miss 68% of the regulators affecting switching rates (Table S5 Comparison 5). We consider differential expression data in

comparison to the set of 191 mutants with white-to-opaque switching rates and the set of 188 mutants with opaque-to-white switching rates as Comparisons 6-9 in Table S5.

Comparisons between switching rates and binding of known regulators in white and opaque cells

We now consider comparisons between switching rates and binding by the known regulators of white-opaque switching in both the white and the opaque cell types. The comparison in the main text (also Table S5, Comparisons 10 and 12) uses the list of 193 mutants with white-to-opaque or opaque-to-white switching data in at least one direction (in other words, without limiting the comparisons only to strains with switching rates in both directions). This set excludes TF59 (*ace2*), TF117 (*tup1*), and TF125 (*nrg1*). As a threshold, we use binding by at least one of the known regulators, taken from previously published ChIP-chip and ChIP-seq experiments (Zordan *et al.* 2007; Hernday *et al.* 2013, 2016; Lohse *et al.* 2013; Lohse and Johnson 2016). We evaluate binding in white cells and binding in opaque cells separately for the purposes of this analysis.

We first consider regulator binding in white cells, where binding events are found upstream of 29 of the 193 regulators (Table S5 Comparison 10). As noted above, there are 26 (out of 193) regulators that have at least a 10-fold effect on switching in one direction and seven of these (27%, 7/26) are bound by one or more regulators in white cells. This represents 24% of the 29 regulators (7/29) that are bound by one or more of the known "core" regulators in white cells. This represents a 1.8-fold improvement on what would have been expected by chance, is not significant (4.64e-2), and fails to predict 73% of the mutants affecting switching rates 10-fold.

There are 59 (out of 193) regulators with at least a three-fold effect on switching in one direction (Table S5 Comparison 11). Thirteen of these (22%, 13/59) are bound by one or more regulators in white cells, representing 45% of the 29 regulators (13/29) bound by one or more regulators in white cells. This is a 1.5-fold improvement over what would have been expected by chance, is not significant (3.49e-2), and misses 78% of mutants with three-fold effects on switching rates.

We now consider opaque cells, where the binding events are found upstream of 64 out of the 193 regulators (Table S5 Comparison 12). There are 26 (out of 193) regulators that have at least a 10-fold effect on switching in one direction. Nine of these (35%, 9/26) are bound by one or more regulators in opaque cells. This represents only 14% of the 64 regulators (9/64) that are bound by one or more regulators in opaque cells. This is only a 1.04-fold improvement on what would have been expected by chance, is not significant (1.73e-1), and fails to predict 65% of the regulators with 10-fold effects on switching rates.

There are 59 (out of 193) regulators that have at least a three-fold effect on switching in one direction (Table S5 Comparison 13). 22 of these (37%, 22/59) are bound by one or more regulators in opaque cells. This represents 34% of the 64 regulators (22/64) that are bound by one or more regulators in opaque cells. This represents a 1.1-fold improvement on what would have been expected by chance, is not significant (9.42e-2), and misses 63% of the regulators that affect switching rates three-fold.

In order to directly evaluate correlation between switching rates and binding events, we have calculated correlation independently for the 191 mutants with white-to-opaque switching rates and the 188 mutants with opaque-to-white switching rates. As before, these comparisons treat white cell binding and opaque cell binding separately for this analysis. We do not observe

an obvious correlation between switching in either direction and binding in either cell type as the Pearson correlation coefficient ranges between 0.18 and -0.04 while the Spearman rank correlation coefficient ranges between 0.14 and -0.13. Although we have not discussed these comparisons in detail, they are included in Table S5 as Comparisons 14-21. For these correlation calculations, we have assigned a value between 0 and 8 to each mutant depending on the number of distinct core regulators that bind to it in each cell type. We note that analyses where binding was scored as a binary value (where 0 represents nothing bound and 1 represents 1 to 8 regulators bound) gave similar results.

Growth Rate Effects

Growth rate assays were performed for white cell isolates of 194 mutants. The TF113 (*rbf1*) and TF121 (*ssn6*) mutants are not part of this list due to the lack of white colonies, however we did measure growth for the TF117 (*tup1*), TF125 (*nrg1*), and TF59 (*ace2*). As we do not have white-to-opaque switching frequencies for these strains, they are excluded when comparing switching rates and growth rates, leaving 191 mutants in those cases (Figure 3A). We have defined a growth rate defect as a 20% reduction relative to wild type growth, 14 white strains (15 if TF125 (*nrg1*) is included) have a defect of this amount.

Growth rate assays were performed for opaque cell isolates of 187 mutants. The TF56 (*wor2*), TF59 (*ace2*), TF117 (*tup1*), TF125 (*nrg1*), TF175 (*flo8*), TF176 (*wor1*), and TF181 (*wor4*) mutants were excluded due to a lack of opaque cells. TF137 (*bcr1*) was excluded due to opaque hyperfilamentation issues. Although we could obtain opaque colonies for TF152 (*fgr15*), the increased opaque-to-white switching exhibited by this strain resulted in white cells eventually becoming dominant in liquid culture. As such, we could not measure the opaque cell growth rate

for TF152. All of the remaining 187 mutants have opaque-to-white switching frequencies (Figure 3B, Table S5 Comparisons 25-27). Using the 20% growth reduction threshold, we find 18 opaque mutants with growth rate defects (20 if TF113 (*rbf1*) and TF121 (*ssn6*) are included).

White cell growth rates and white-to-opaque switching rates comparison

We focus on growth defects greater than 20% for this analysis. As noted above, we have both white-to-opaque switching rates and white cell growth rates for 191 mutants (Figure 3A, Table S5 Comparisons 22-24). Of the 20 mutants affecting white-to-opaque switching at least 10-fold, 40% (8/20) also exhibited a white cell growth defect. This represents 57% (8/14) of the mutants with a slow white cell growth phenotype and is a 5.5-fold enrichment over what would be expected by chance. This effect is significant (6.61e-06), however it fails to account for 60% of the mutants affecting the white-to-opaque switching rate. If we consider mutants with a three-fold effect on white-to-opaque switching, 31% (13/42) also have a growth rate defect. This represents 93% of the mutants with a slow white cell growth phenotype (13/14) and is a 4.2-fold enrichment over what would be expected by chance. This enrichment is also significant (6.28e-9), however it fails to predict 69% of the mutants with a three-fold effect on white-to-opaque switching. The Pearson correlation coefficient r is -0.29 and the Spearman rank correlation coefficient rho is 0.21, suggesting that any correlation between these two data sets is weak.

If we look specifically at mutants with a five-fold increase in white-to-opaque switching rates, we find that five of the 10 (50%) exhibited a white cell growth defect. This represents 36% of the mutants with a slow white cell growth phenotype and is a 6.8-fold enrichment over what would be expected by chance. This effect is significant (1.95e-04), however it fails to account for 50% of the mutants that increased the white-to-opaque switching rate five-fold (Table S5

Comparison 28). If we look specifically at mutants with a five-fold decrease in white-to-opaque switching rates, we find that six of the 21 (29%) exhibited a white cell growth defect. This represents 43% of the mutants with a slow white cell growth phenotype and is a 3.9-fold enrichment over what would be expected by chance. This effect is significant (1.31e-03), however it fails to account for 71% of the mutants that decreased the white-to-opaque switching rate five-fold (Table S5 Comparison 29).

Opaque cell growth rates and opaque-to-white switching rates comparison

We focus on growth defects greater than 20% for this analysis. As noted above, we have both opaque-to-white switching rates and opaque cell growth rates for 187 mutants (Figure 3B, Table S5 Comparisons 25-27). Of the nine mutants affecting opaque-to-white switching at least 10-fold, 56% (5/9) also exhibited an opaque cell growth defect. This represents 25% (5/20) of the mutants with a slow opaque cell growth phenotype and is a 5.2-fold enrichment over what would be expected by chance. This effect is significant (7.65e-04) and is one of the most predictive we observed as it only misses 44% of the mutants affecting the opaque-to-white switching rate. Considering mutants with a three-fold effect on opaque-to-white switching, we find that 36% (10/28) also have an opaque growth defect. This represents 50% (10/20) of the mutants with a slow opaque cell growth phenotype and is a 3.3-fold enrichment over what would be expected by chance. This effect is significant (7.14e-05), however expanding the number of mutants means that opaque growth defects now miss 64% of the mutants affecting the opaque-to-white switching rate. The Pearson correlation coefficient r is 0.21 and the Spearman rank correlation coefficient rho is 0.21, suggesting that any correlation between these two data sets is weak.

There are no mutants with a five-fold increase in opaque-to-white switching rates to consider (Table S5 Comparison 30). If we look specifically at mutants with a five-fold decrease in opaque-to-white switching rates, we find that seven of the 15 (47%) exhibited an opaque cell growth defect. This represents 35% of the mutants with a slow white cell growth phenotype and is a 4.4-fold enrichment over what would be expected by chance. This effect is significant (1.91e-04), however it fails to account for 53% of the mutants that decreased the white-to-opaque switching rate five-fold (Table S5 Comparison 31).

White growth rate and opaque growth rate comparisons

We have both white cell and opaque cell growth rates for 185 strains and used these 185 strains when comparing white and opaque growth rates in the Results (Figure 3C, Table S5 Comparison 32). This set excludes TF59 (*ace2*), TF117 (*tup1*), and TF125 (*nrg1*). It also excludes TF113 (*rbf1*) and TF121 (*ssn6*) due to a lack of white cells and TF56 (*wor2*), TF175 (*flo8*), TF176 (*wor1*), and TF181 (*wor4*) due to a lack of opaque cells. TF137 (*bcr1*) was excluded due to opaque hyperfilamentation issues. TF152 (*fgr15*) was also excluded due to issues noted above. Focusing on this set of mutants at the 20% growth rate defect threshold, we find 14 mutants with a white cell growth defect and 18 with an opaque cell growth defect. Seven of the mutants affect both cell types, giving a total of 25 mutants affecting growth. The overlap represents 50% of the white cell mutants (7/14) and 39% of the opaque cell mutants (7/18). This represents a 5.1-fold enrichment over what would be expected by chance and is significant (5.28e-5), however we note that growth rate defects in the opposite cell type would fail to predict 50% of white cell growth defects and 61% of opaque cell growth defects. These data sets have

the best correlation we observed, with a Pearson correlation coefficient r of 0.54 and a Spearman rank correlation coefficient rho of 0.38.

Statistical Analysis of the Growth Rate Assays

As discussed above, we used Welch's t-test (two-tailed) to compare the growth rates of mutant strains to the wild type controls from the same day (usually three wells of each). We have included three strains excluded from our broader analyses due to the lack of growth rates in both cell types (TF125/*nrg1* in white cells only, TF113/*rbf1* and TF121/*ssn6* in opaque cells only). We note that the raw p-values (before correcting for multiple comparisons) are less than 0.01 for all but one of the white cell mutants (TF036/*hcm1*) and all of the opaque cell mutants with 20% growth defects. The raw p-values are less than 0.001 for nine of the 15 white cell mutants and 16 of the 20 opaque cell mutants with 20% growth defects. The raw p-values generated from this analysis are included in File S2, columns AA and AD.

Due to the large number of comparisons made (194 for white cell growth rates and 187 for opaque cell growth rates), it is necessary to correct for the multiple comparisons. To do this, we performed the Benjamini-Hochberg procedure (BH step-up procedure) with $\alpha = 0.05$. We find that 14 of 15 mutants (all but TF036/*hcm1*) with 20% growth defects in white cells and all mutants with 20% growth defects in opaque cells are significant at this threshold. We have indicated the mutants that were significant at $\alpha = 0.05$ for both growth rate assays in File S2, columns AB and AE.

Literature Cited

Hernday, A. D., M. B. Lohse, P. M. Fordyce, C. J. Nobile, J. D. DeRisi *et al.*, 2013 Structure of the transcriptional network controlling white-opaque switching in *Candida albicans*. Mol. Microbiol. 90: 22–35.

Hernday, A. D., M. B. Lohse, C. J. Nobile, L. Noiman, C. N. Laksana *et al.*, 2016 Ssn6 defines a new level of regulation of white-opaque switching in *Candida albicans* and is required for the stochasticity of the switch. MBio 7: e01565–15.

Lohse, M. B., A. D. Hernday, P. M. Fordyce, L. Noiman, T. R. Sorrells *et al.*, 2013 Identification and characterization of a previously undescribed family of sequence-specific DNA-binding domains. Proc. Natl. Acad. Sci. U. S. A. 110: 7660–7665.

Lohse, M. B., and A. D. Johnson, 2016 Identification and Characterization of Wor4, a New Transcriptional Regulator of White-Opaque Switching. G3 6: 721–9.

Tuch, B. B., Q. M. Mitrovich, O. R. Homann, A. D. Hernday, C. K. Monighetti *et al.*, 2010 The transcriptomes of two heritable cell types illuminate the circuit governing their differentiation. PLoS Genet. 6: e1001070.

Zordan, R., M. Miller, D. Galgoczy, B. Tuch, and A. Johnson, 2007 Interlocking transcriptional feedback loops control white-opaque switching in *Candida albicans*. PLoS Biol. 5: e256.

File S2: Compilation of switching frequency and growth rate data from this study. For columns F, H through S, V, Y, AB, and AE, a "1" represents yes and/or inclusion in that set. For columns T to AE, cells were left blank if it was not possible to measure a value for that strain in a given assay. From left to right in the Excel spreadsheet, columns are as follows. (A) Transcriptional regulator number assigned for this study. (B) Orf19 number designation based on the Candida Genome Database (CGD). (C) Current CGD systematic name for the gene. (D) Gene name, where applicable. (E) List of regulators that may have been left out of different analyses with indication of the reasons for this. See File S1 for more details. (F) Previously known regulators of white-opaque switching. (G) List of the 12 regulator mutants with opaque cellular morphologies discussed in this study. (H) List of regulators with at least a 10-fold effect on switching rates in either the white-to-opaque or opaque-to-white directions. (I) List of regulators with at least a five-fold effect on switching rates in either the white-to-opaque or opaque-to-white directions. (J) List of regulators with at least a three-fold effect on switching rates in either the white-to-opaque or opaque-to-white directions. (K) List of regulators with at least a 10-fold effect on white-to-opaque switching rates. (L) List of regulators with at least a five-fold effect on white-to-opaque switching rates. (M) List of regulators with at least a three-fold effect on white-to-opaque switching rates. (N) List of regulators with at least a 10-fold effect on opaque-to-white switching rates. (O) List of regulators with at least a five-fold effect on opaque-to-white switching rates. (P) List of regulators with at least a three-fold effect on opaque-to-white switching rates. (Q) List of regulators with at least a 20% reduction in growth rate relative to wild type in either cell type. (R) List of regulators with at least a 20% reduction in growth rate relative to wild type in the white cell type. (S) List of regulators with at least a 20% reduction in growth rate relative to wild type in the opaque cell type. (T) White-to-opaque switching frequency, normalized to the average of five wild type switching assays performed the same day. When no switching events were detected for a strain in the screen, the switching frequency is indicated as one divided by the number of colonies counted. (U) Statistical evaluation of the significance of difference in

white-to-opaque switching rates relative to wild type rates. Raw p-value for two-tailed Welch's t-test (unequal variances t-test). (V) Whether the white-to-opaque switching rate was significantly different from the wild type rate following the Benjamini-Hochberg procedure with $\alpha = 0.05$. (W) Opaque-to-white switching frequency, normalized to the average of five wild type switching assays performed the same day. When no switching events were detected for a strain in the screen, the switching frequency is indicated as one divided by the number of colonies counted. (X) Statistical evaluation of the significance of difference in opaque-to-white switching rates relative to wild type rates. Raw p-value for two-tailed Welch's t-test (unequal variances t-test). (Y) Whether the opaque-to-white switching rate was significantly different from the wild type rate following the Benjamini-Hochberg procedure with $\alpha = 0.05$. (Z) Maximum growth rate in white cells, normalized to the maximum growth rate of the wild type strain on the same day. (AA) Statistical evaluation of the significance of difference in mutant white cell growth rates relative to wild type growth rates. Raw p-value for two-tailed Welch's t-test (unequal variances t-test). (AB) Whether the mutant white cell growth rate was significantly different from the wild type growth rate following the Benjamini-Hochberg procedure with $\alpha = 0.05$. (AC) Maximum growth rate in opaque cells, normalized to the maximum growth rate of the wild type strain on the same day. (AD) Statistical evaluation of the significance of difference in mutant opaque cell growth rates relative to wild type growth rates. Raw p-value for two-tailed Welch's t-test (unequal variances t-test). (AE) Whether the mutant opaque cell growth rate was significantly different from the wild type growth rate following the Benjamini-Hochberg procedure with $\alpha = 0.05$. (AF) Previously published RNA-seq of opaque versus white cells; values are on a $\log_2$ scale (Tuch *et al.* 2010). (AG) Number of regulators bound at the control region of the gene in white cells, based on previously published ChIP-chip and ChIP-seq studies (Hernday *et al.* 2013, 2016; Lohse and Johnson 2016). (AH) Number of regulators bound at the control region of the gene in opaque cells, based on previously published ChIP-chip and ChIP-seq studies (Zordan *et al.* 2007; Hernday *et al.* 2013, 2016; Lohse *et al.* 2013; Lohse and Johnson 2016). (.xlsx, 61 KB)

Available for download as a .xlsx file as:

http://www.genetics.org/lookup/suppl/doi:10.1534/genetics.116.190645/-/DC1/FileS2.xlsx